CHAPTER IV

RESULTS AND DISCUSSION

The hexadentate Schiff base metal complexes were synthesized following the synthetic route as described in the literature [24]. The reaction between 2,4-dihydroxybenzaldehyde and metal (II) acetate in methanol to form a template intermediate subsequently, the solution of triethylenetetramine was then added to obtain ZnL and NiL (Scheme 4.1)

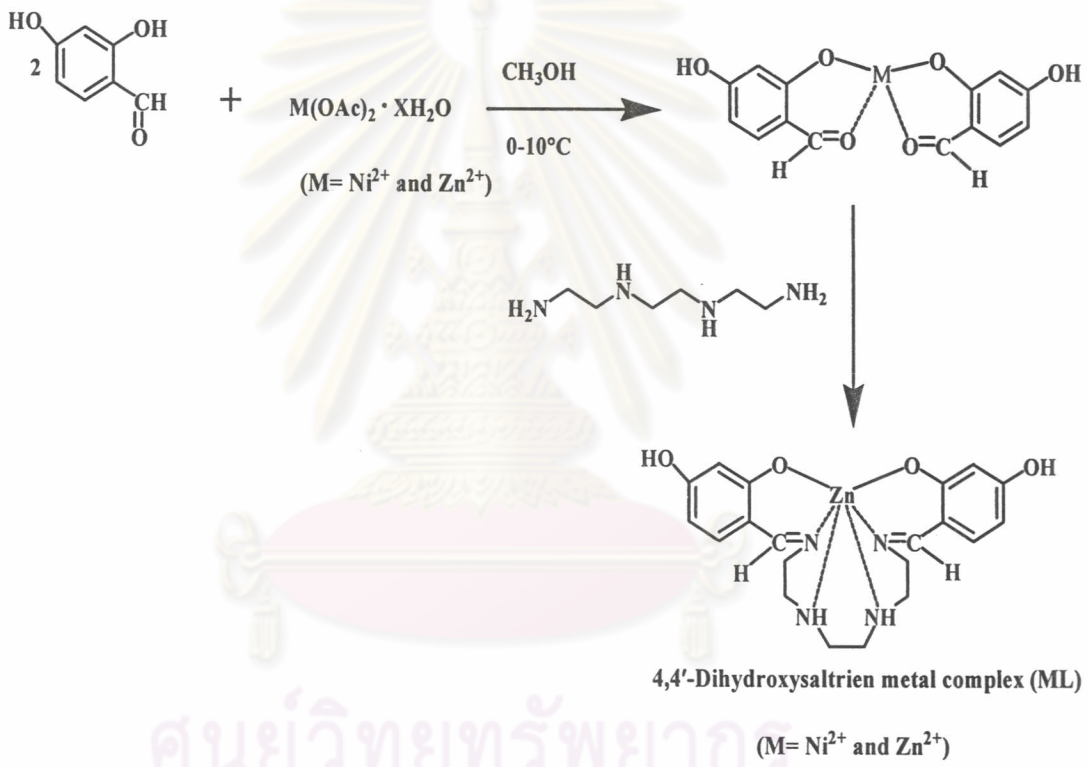

4,4′-Dihydroxysaltrien metal complex (ML)

(M= Ni^{2+} and Zn^{2+})

ศูนย์วิทยทรัพยากร
จุฬาลงกรณ์มหาวิทยาลัย

Scheme 4.1 Synthesis of 4,4′- dihydroxysaltrien metal complexes (ML)

4.1 Synthesis of hexadentate Schiff base metal complexes (ML)

4.1.1 Synthesis and characterization of 4,4′-dihydroxysaltrien zinc-complex (ZnL)

ZnL was synthesized following the synthetic route as described in the literature [24]. ZnL was also synthesized by adding triethylenetetramine to a mixture of zinc (II) acetate and 2,4-dihydroxybenzaldehyde at the mole ratio of triethylenetetramine: zinc (II) acetate:2,4-dihydroxybenzaldehyde = 1:1:2. After the complex formation was completed, the reaction mixture was neutralized by addition of potassium carbonate solution. The pink powder, which was the by-products, precipitated immediately and was separated by filtration. The filtrate was allowed to stand at temperature for 4 to 6 hours and the yellow crystal of ZnL was obtained. ZnL are soluble in dimethyl formamide (DMF) and dimethy sulfoxide (DMSO) but insoluble in tetrahydrofuran, methanol, chloroform, dichloromethane, acetonitride.

The structure of ZnL was confirmed by spectroscopic methods and the data agreed with those reported in the literature [24]. IR spectrum (Figure 4.1) of ZnL showed important bands as follows: 3315 cm^{-1} (N-H stretching), 1632 cm^{-1} (C=N stretching), 1548 cm^{-1} (aromatic C=C stretching), 1218 cm^{-1} (aromatic C-C stretching), 983 and 843 cm^{-1} (C-H bending of 1, 2, 4-trisubstituted benzene).

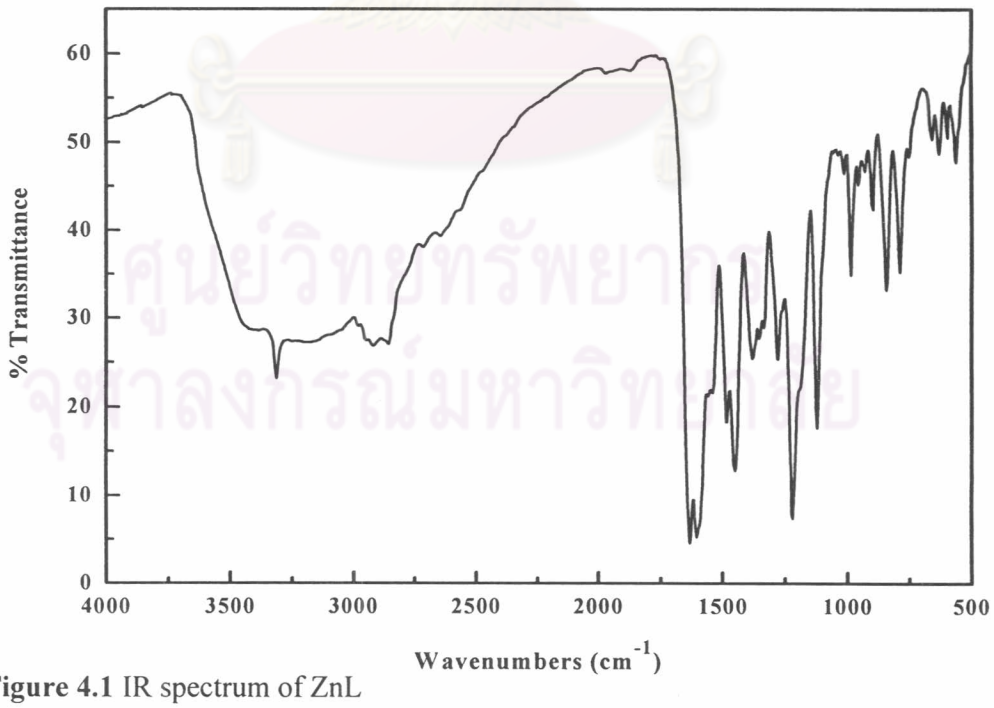

Figure 4.1 IR spectrum of ZnL

Additionally, ^{1}H and ^{13}C NMR data (Figures 4.2-4.3 and Table 4.1) of ZnL also supported its structure. ^{1}H and ^{13}C NMR spectra showed the characteristic imine –CH=N- protons at 8.10 ppm and carbons of ZnL at 166 ppm, respectively.

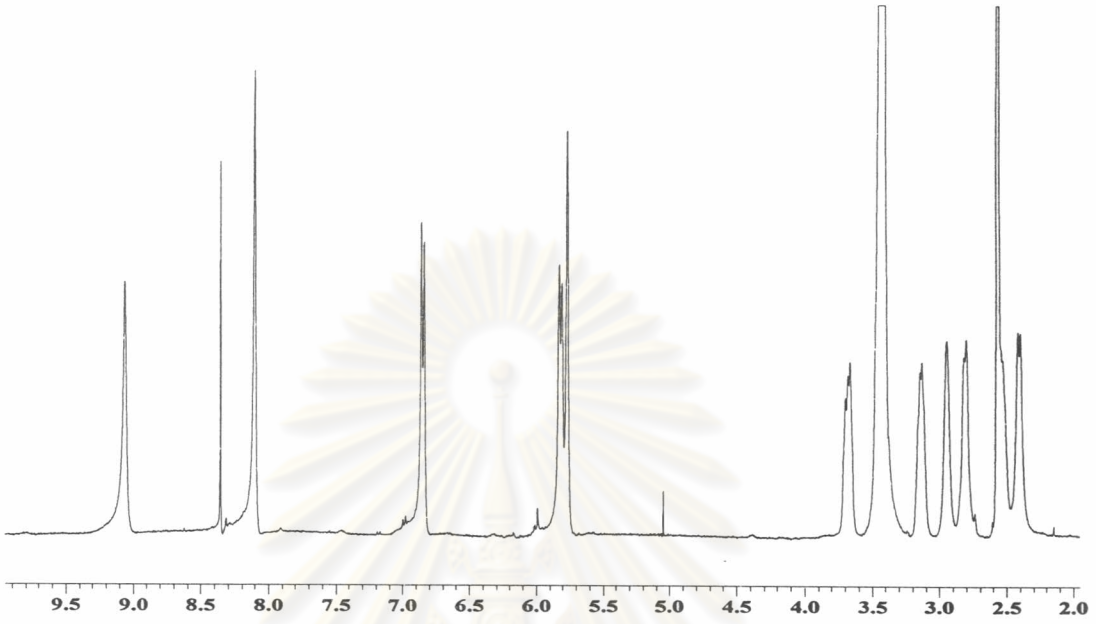

Figure 4.2 ^{1}H-NMR spectrum of ZnL in DMSO-d_6

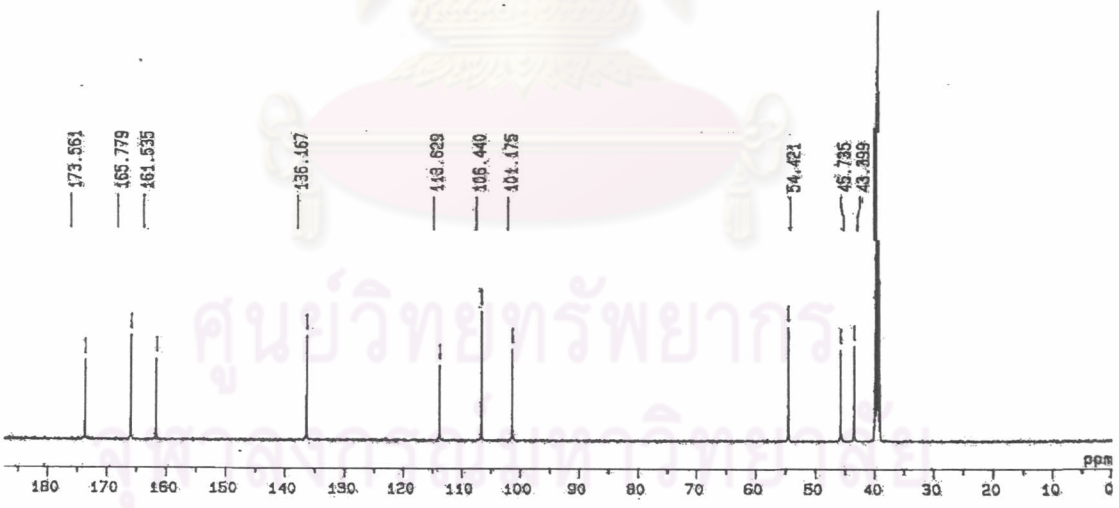

Figure 4.3 ^{13}C-NMR spectrum of ZnL in DMSO-d_6

Table 4.1 Assignment of ^{1}H and ^{13}C NMR data of ZnL

^{1}H NMR signals				^{13}C NMR signals		
-CH=N	Ar-H	-OH	$-CH_2$	-CH=N	Ar-H	$-CH_2$
8.10	6.85 (d, 2H) 5.82 (d, 2H) 5.77 (s, 2H)	9.06 (s, 2H)	3.70-3.66 (m, 2H) 3.14-3.13 (m, 2H) 2.94 (s, 2H) 2.80 (d, 2H) 2.54-2.53 (m, 2H) 2.40 (d, 2H)	165.78	173.56, 161.54 136.17, 113.63 106.44, 101.17	54.42, 45.74,43.40

Comparing between the structure of ZnL and $ZnSal_2trien$ (Figures 4.4a and b respectively), ZnL complex contains additional two hydroxyl groups. From our previous work, the X-ray crystal structure of $ZnSal_2trien$ was obtained [25]. The geometry of $ZnSal_2trien$ is distorted octahedron (Figure 4.4c). The Zn (II) atom is coordinated by two oxygen atoms, two imine nitrogen atoms and two amine nitrogen atoms. Therefore, it is possible the geometry of ZnL is also octahedron with the same coordination as in the case of $ZnSal_2trien$.

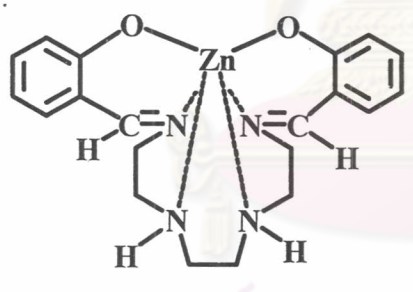

(a) $ZnSal_2trien$

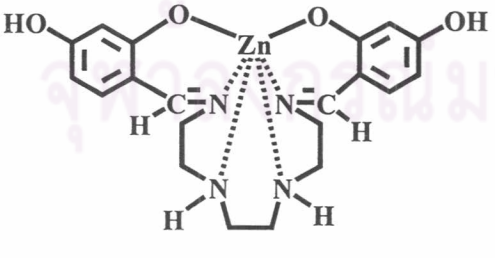

(b) ZnL

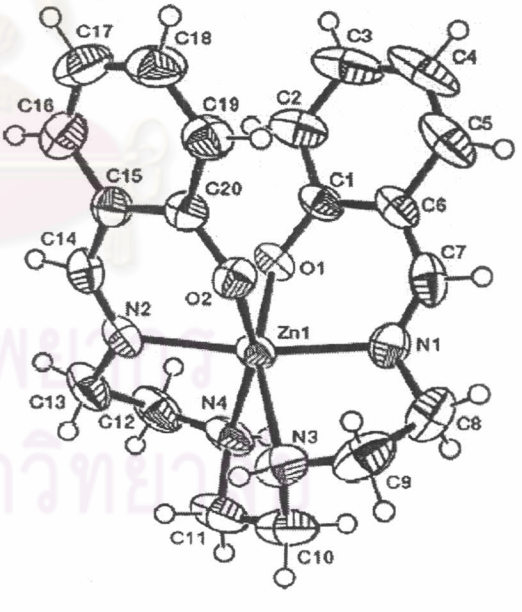

(c) X-ray crystal structure of $ZnSal_2trien$

Figure 4.4 (a) $ZnSal_2trien$; (b) ZnL; (c) X-ray crystal structure of $ZnSal_2trien$

4.1.2 Synthesis and characterization of 4,4′-dihydroxysaltrien nickel complex (NiL)

NiL was synthesized following the synthetic route described in 4.1.1 employing the mole ratio of triethylenetetramine: nickel (II) acetate: 2,4-dihydroxybenzaldehyde = 2:1:2. In the neutralization step, the pink powder precipitated immediately and was isolated by filtration. The filtrate was allowed to stand at room temperature for 4 hours and the green crystal of NiL was obtained. NiL was soluble in dimethyl formamide (DMF) and dimethyl sulfoxide (DMSO) but insoluble in tetrahydrofuran, methanol, chloroform, dichloromethane, acetonitride.

NiL structure was confirmed using IR and the data agreed with those reported in the literature [24]. The IR spectrum (Figure 4.5) showed the important bands as follows: 3314 cm^{-1} (N-H stretching), 1634 cm^{-1} (C=N stretching), 1559 cm^{-1} (aromatic C=C stretching), 1215 cm^{-1} (aromatic C-C stretching), 988 and 840 cm^{-1} (C-H bending of 1, 2, 4-trisubstituted benzene).

ศูนย์วิทยทรัพยากร
จุฬาลงกรณ์มหาวิทยาลัย

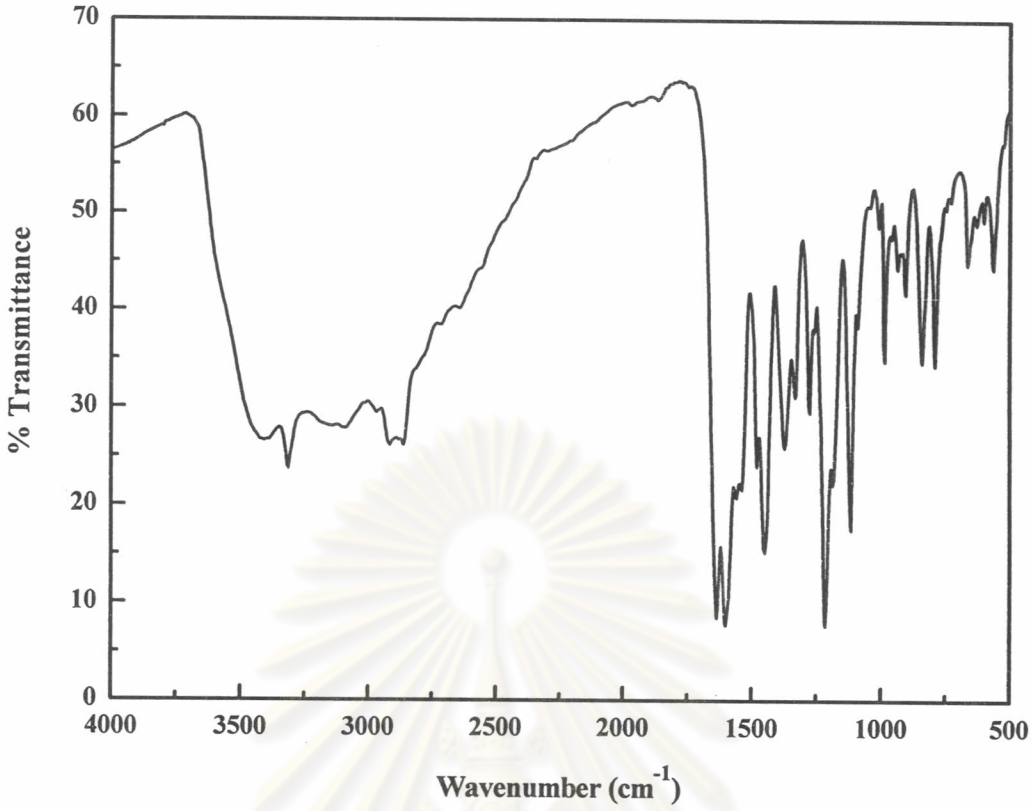

Figure 4.5 IR spectrum of NiL

4.1.3 Thermal property of ZnL and NiL

Thermal stability of the complexes was investigated by using of TGA. TGA thermograms of ZnL and NiL are displayed in Figure 4.6. Weight loss percentages of metal complexes at different temperatures and initial decomposition temperatures (IDT) are given in Table 4.4.

ศูนย์วิทยทรัพยากร
จุฬาลงกรณ์มหาวิทยาลัย

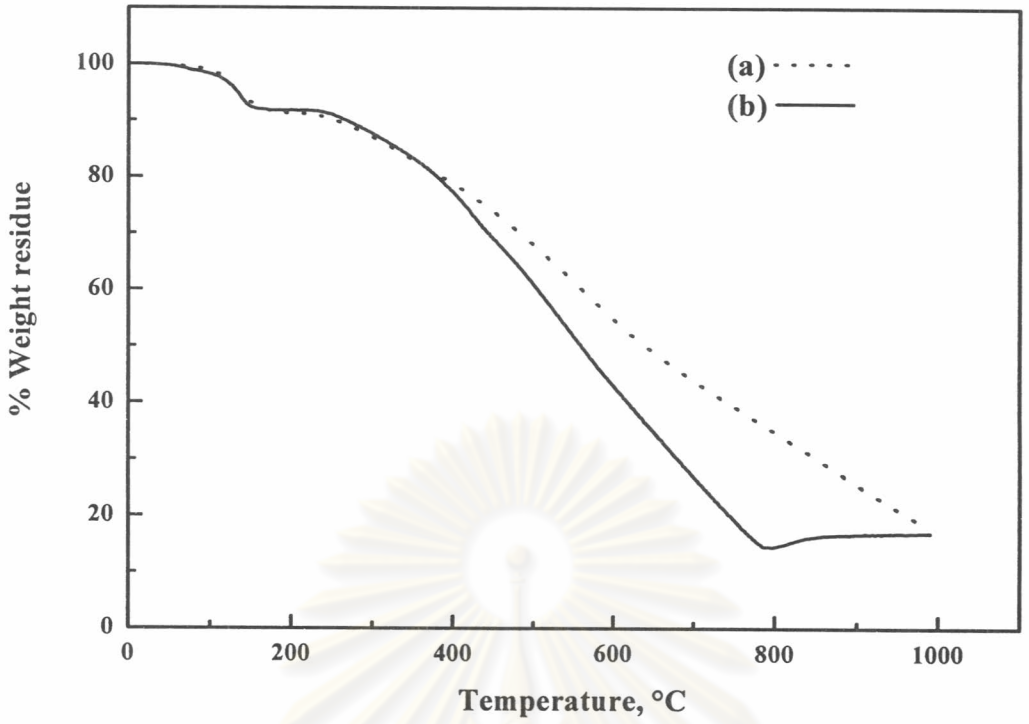

Figure 4.6 TGA thermogram of (a) ZnL (b) NiL

Table 4.2 TGA data of ZnL and NiL

Metal complexes	IDT (°C)	Weight loss (%) at different temperature (°C)							% Metal oxide
		300	400	500	600	700	800	900	
ZnL	106.4	13	21	32	45	56	65	74	18
NiL	105.2	12	13	39	57	73	85	83	17

Both ZnL and NiL had 10 % weight loss at the same temperature. The first stage of decomposition probably involved the loss of H_2O in the metal complex crystals. At the temperature above 400°C, NiL had higher weight loss percentage than ZnL. This indicated that, ZnL was more thermally stable than NiL. After the metal complexes decomposed at high temperature, the theoretical amount of ZnO and NiO formed should be 17% and 16%, respectively, which roughly corresponded to amount obtained from TGA experiments.

4.1.4 UV-visible spectroscopy of ZnL and NiL

Figure 4.7 shows the UV-visible spectra of the metal complexes. From these figures, ZnL had two absorption bands while NiL showed one absorption band.

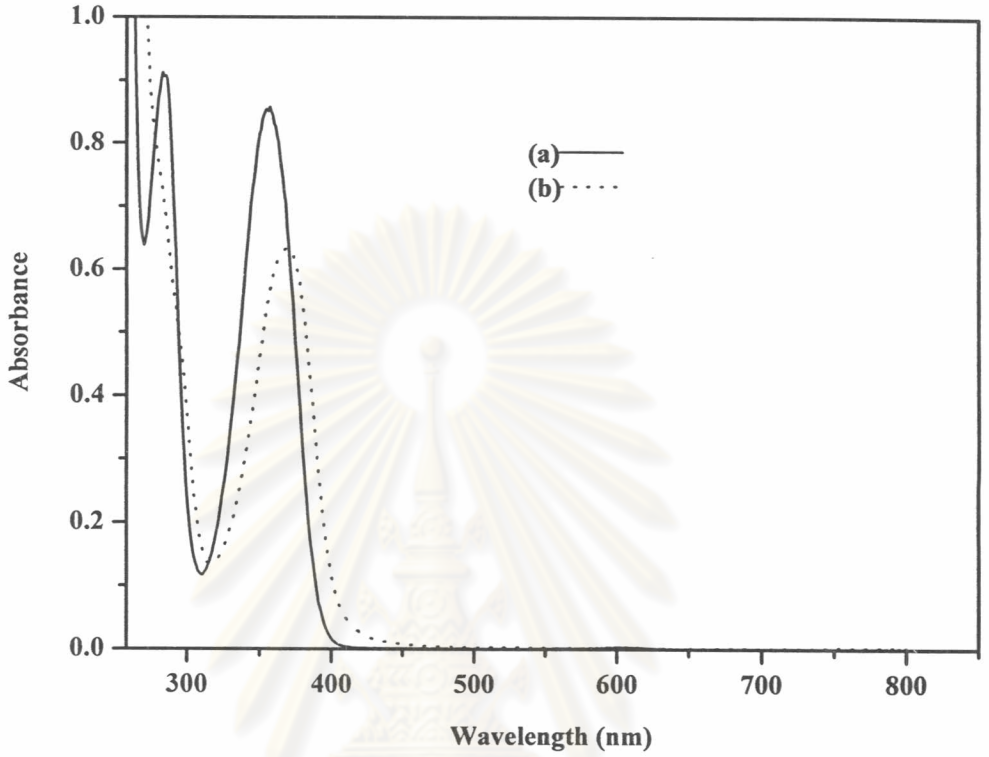

Figure 4.7 UV-visible spectra of (a) ZnL and (b) NiL

Table 4.3 UV-visible data of the metal complexes in DMSO

Metal complexes	λ_{max} (nm)	Color in DMSO
ZnL	283, 357 ε_1 = 18246.2 cm^{-1} $mol^{-1}dm^3$ ε_2 = 17158.8 cm^{-1} $mol^{-1}dm^3$	Light yellow
NiL	368 ε = 12647.4 cm^{-1} $mol^{-1}dm^3$	Dark green

4.2 Synthesis of metal-containing polyurethane-ureas (ML-PUU)

4.2.1 Synthesis of ML-PUU from the reaction between ML and different diisocyanates

The reaction of ML with different diisocyanates is shown in Scheme 4.2. The metal complexes contain two amino and two hydroxyl groups capable of undergo polymerization with diisocyanate groups to give metal-containing polyurethane-ureas.

The reaction between ML (M = Zn^{2+}, Ni^{2+}) and diisocyanates at a molar ratio of 1:2 was carried out in dried DMSO at 80-90 °C with DBTDL as a catalyst. The yields of zinc- and nickel-containing polyurethane-ureas were in the range of 68-90% and 65-93%, respectively. Zinc- and nickel-containing polyurethane-ureas were obtained as red-orange and red-brown solids, respectively.

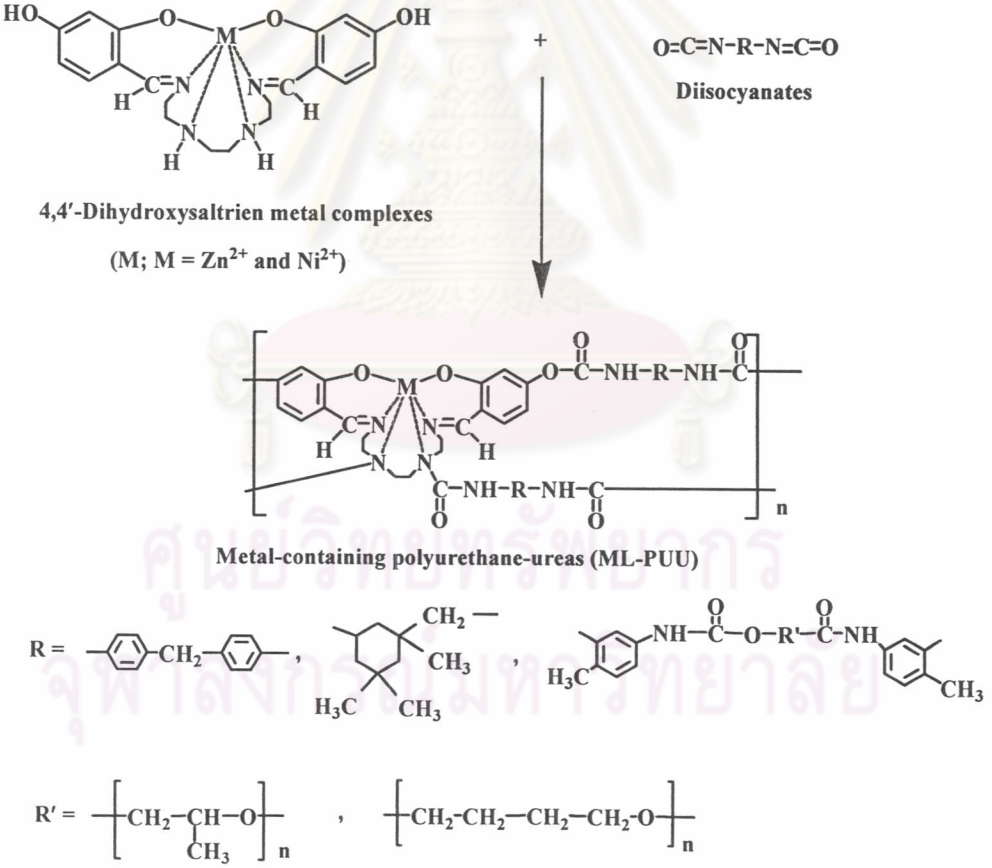

Scheme 4.2 Synthesis of metal-containing polyurethane-ureas (ML-PUU) from the reaction of ML with different diisocyanates.

The possible polymerization mechanism is that the amino and hydroxyl groups in ML undergo reactions with isocyanate groups in diisocyanate compounds to give ureas and urethane linkages, respectively (Scheme 4.3).

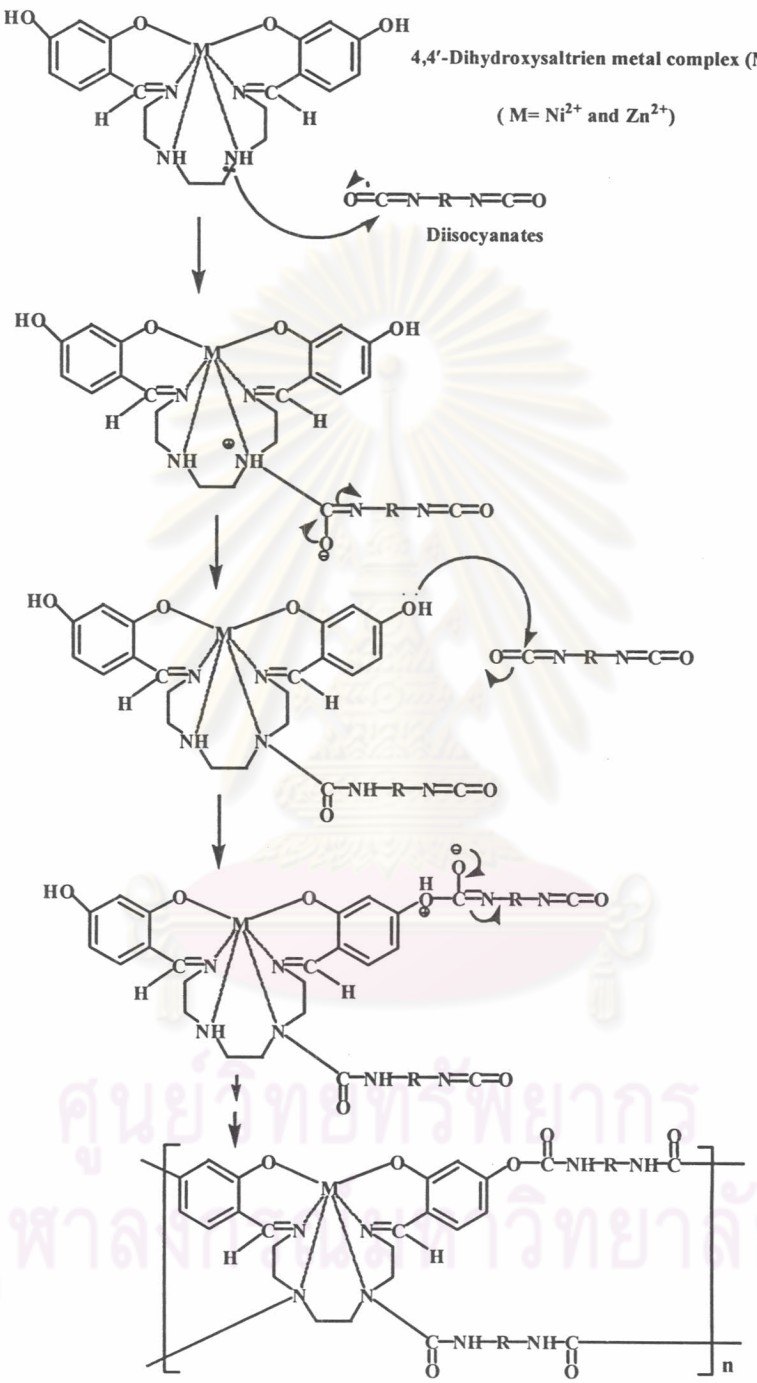

Scheme 4.3 Mechanism of the reaction between ML and diisocyanates to give metal-containing polyurethane-ureas.

4.2.2 Characterization of metal-containing polyurethane-ureas (ML-PUU)

4.2.2.1 IR spectroscopy of ML-PUU

IR spectra of zinc- and nickel-containing polyurethane-ureas are shown in Figures 4.8 and 4.9, respectively. All polymers showed N-H stretching of urea group between 2918-3386 cm^{-1}. The C-H stretching signals appeared between 2974 and 2791 cm^{-1}. The carbonyl (C=O) stretching of urethane and urea in Figure 4.8 (b-c) and Figure 4.9 (b-c) appeared as a shoulder peak between 1688 and 1699 cm^{-1}. The imine (C=N) absorption band in Figure 4.8 (b-c) and Figure 4.9 (b-c) was observed around 1634-1606 cm^{-1}.

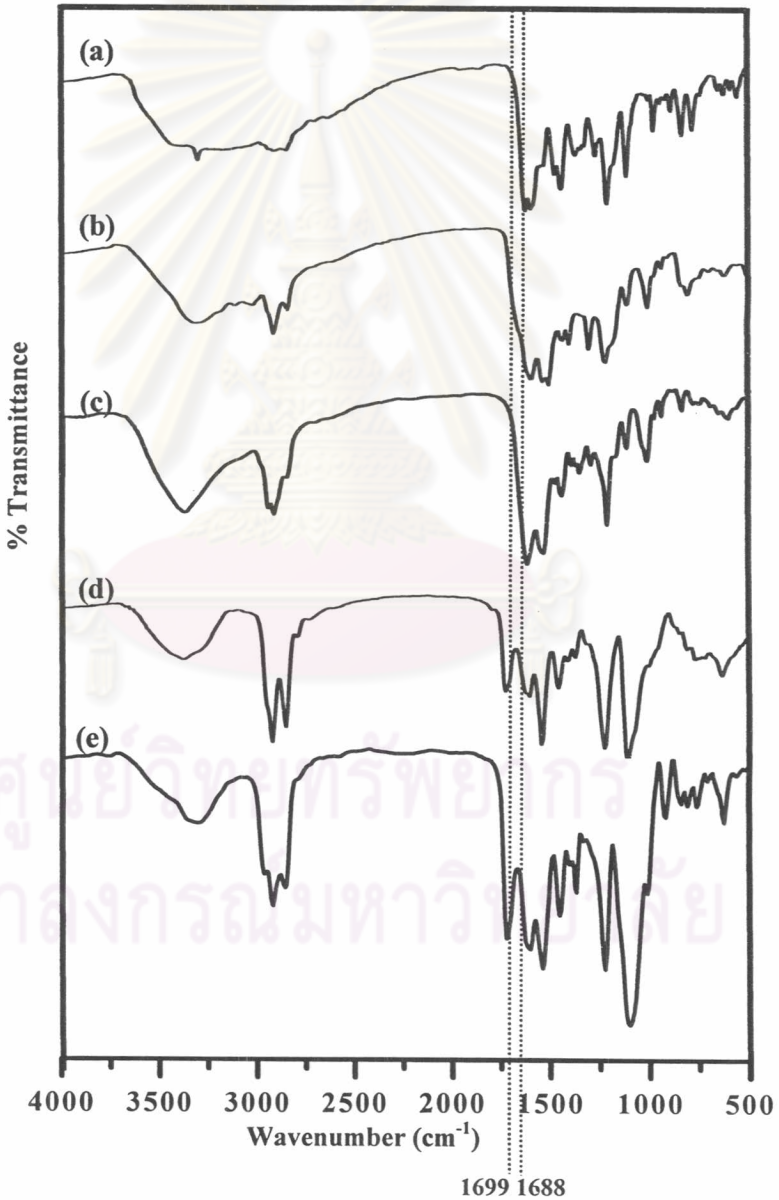

Figure 4.8 IR spectra of zinc-containing polyurethane-ureas: (a) ZnL; (b) ZnL-MDI (1:2); (c) ZnL-IPD (1:2); (d) ZnL-PB (1:2), (e) ZnL-PP (1:2)

From Figures 4.8 (d-e) and 4.9 (d-e), all metal-containing polyurethane-ureas showed carbonyl (C=O) stretching of urethane linkage (-NCOO-) around 1727-1716 cm^{-1} but the carbonyl (C=O) stretching of urea linkage (-NCON-) was not clearly observed due to the overlapping with –C=N- absorption.

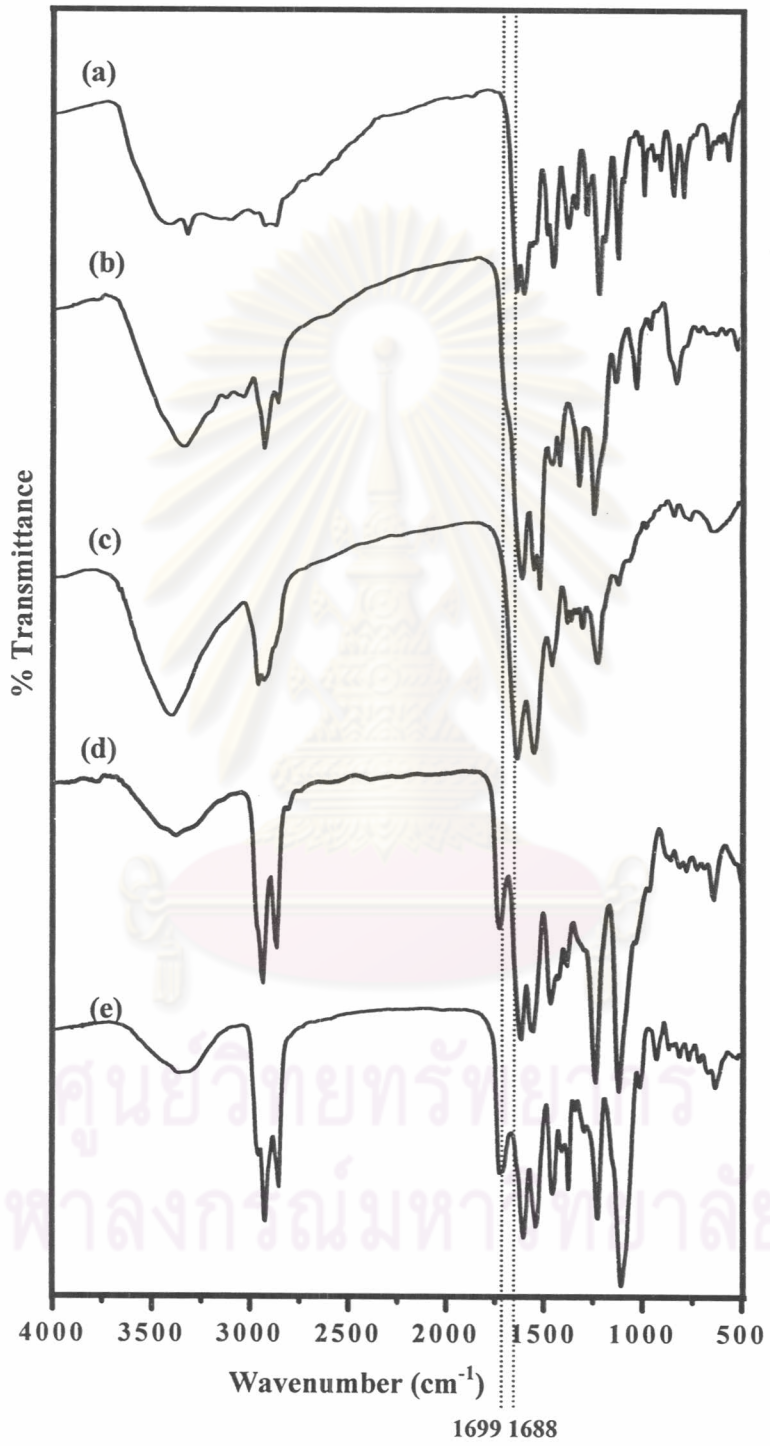

Figure 4.9 IR spectra of nickel-containing polyurethane-ureas: (a) NiL; (b) NiL-MDI (1:2); (c) NiL-IPD (1:2); (d) NiL-PB (1:2), (e) NiL-PP (1:2)

4.2.2.2 NMR Spectroscopy

^{1}H NMR spectrum of zinc-containing polyurethane-ureas (ZnL-MDI (1:2)) in DMSO-d_6 and its characteristic signals are presented in Figures 4.10.

The ^{13}C NMR spectrum of ZnL-MDI (1:2) could not be obtained identified due to the poor solubility of ZnL-MDI (1:2) in DMSO-d_6. ^{1}H NMR spectrum of ZnL-MDI (1:2) showed the characteristic imine -CH=N- proton at δ 8.43. The aromatic protons of ZnL were found at δ 7.23 (s, 2H), 6.87-6.84 (d, 2H, J=8.80 Hz), 6.53-6.51 (d, 2H, J=7.60 Hz). The aromatic protons of MDI were observed at δ 7.35-7.31 (m, 4H) and 7.09-7.04 (m, 4H). The methylene protons of ZnL in the aliphatic region of δ 2.4-3.7 could not be clearly observed due to the overlapping with large peaks of H_2O in DMSO-d_6. Therefore, the chemical shift that could be clearly observed is mainly in the aromatic region.

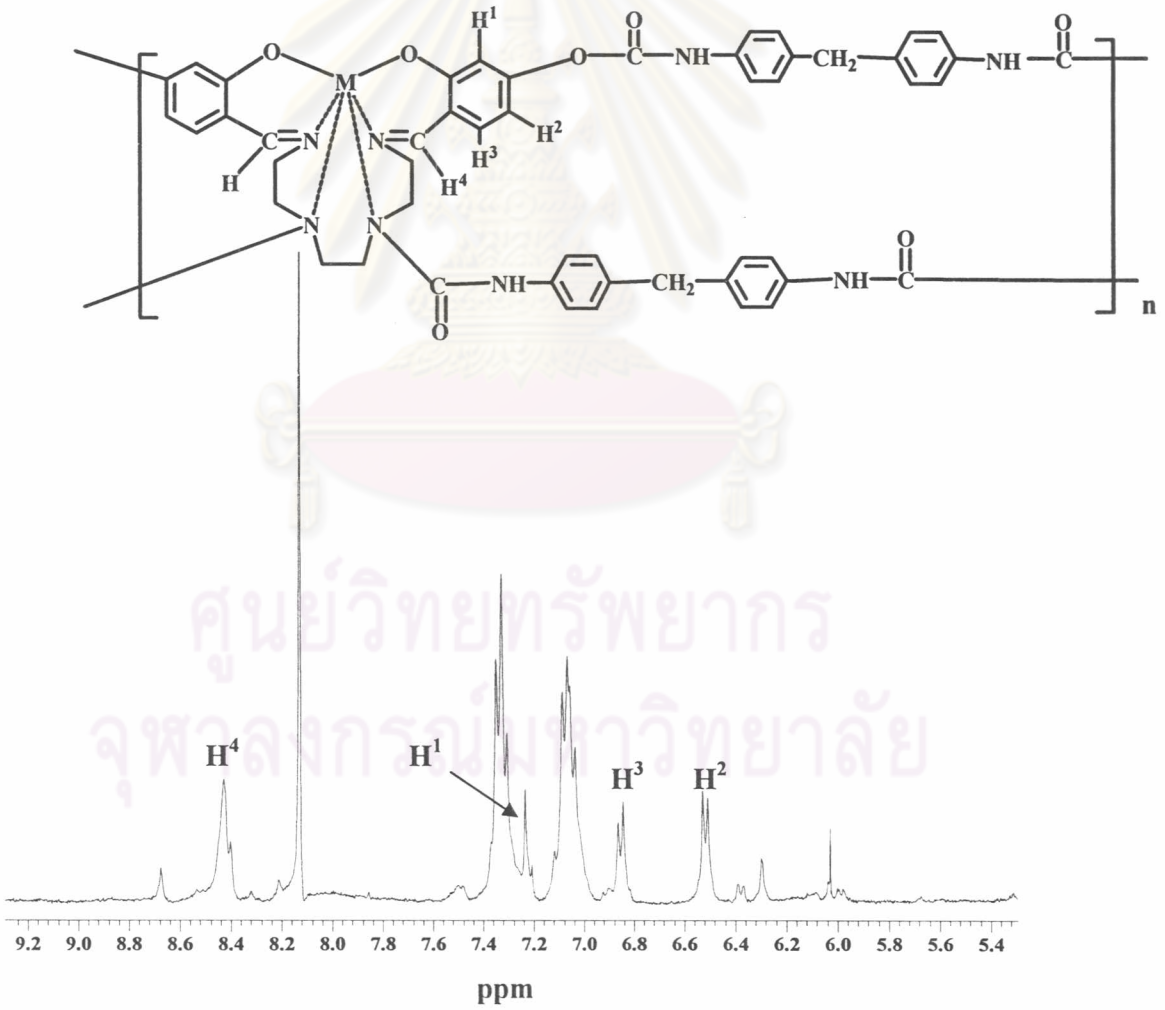

Figure 4.10 ^{1}H NMR spectrum of ZnL-MDI (1:2) in DMSO-d_6

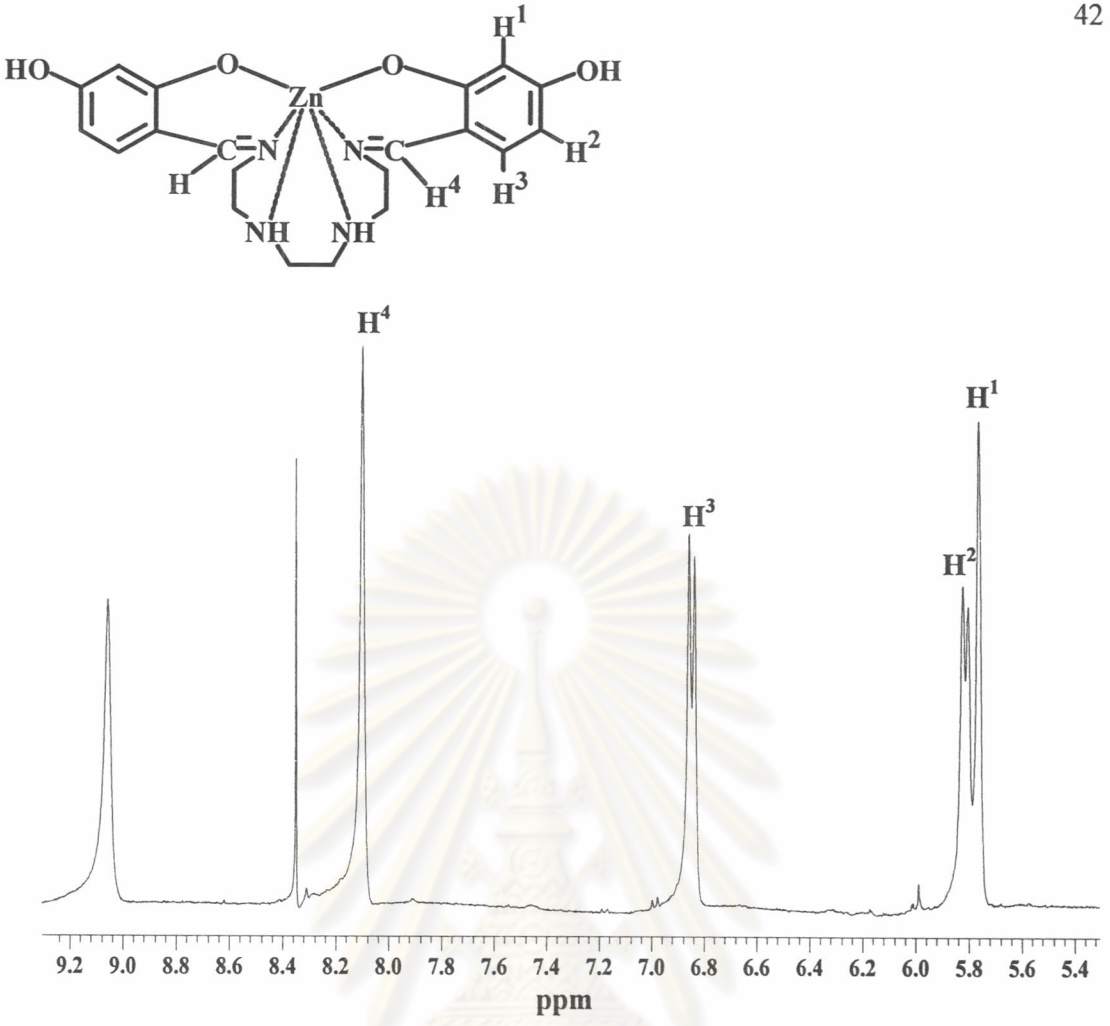

Figure 4.11 ^{1}H NMR spectrum of ZnL in DMSO-d_6

Comparing between the chemical shifts of the same protons on ZnL-MDI (1:2), and ZnL (Figures 4.10 and 4.11, respectively) it was found that they appeared at different positions. The aromatic protons of the ZnL itself (H^1, H^2, H^3) showed resonance signals at δ 5.78-6.88, while these protons in ZnL-MDI (1:2) showed the resonance signals at δ 6.51-7.23 due to the electron withdrawing effect of the carbonyl carbon of urethane group. This effect was obvious in the resonance signal of H^1 in ZnL and ZnL-MDI (1:2), which shifted from δ 5.78 to δ 7.23, respectively. The signal of –C=NH in both ZnL and ZnL-MDI (1:2) also shifted slightly from δ 8.10 to 8.43, respectively.

Therefore, the above data from ^{1}H NMR supported the structure of ZnL-MDI (1:2), which was a linear chain polymer, as shown in Figure 4.12. However, there was another possible structure of ZnL-MDI (1:2), which was a crosslinked polymer, as shown in Figure 4.13.

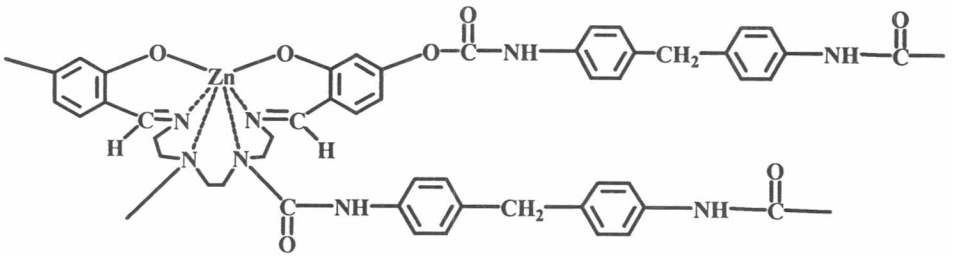

Figure 4.12 Possible linear chain structure of ZnL-MDI (1:2)

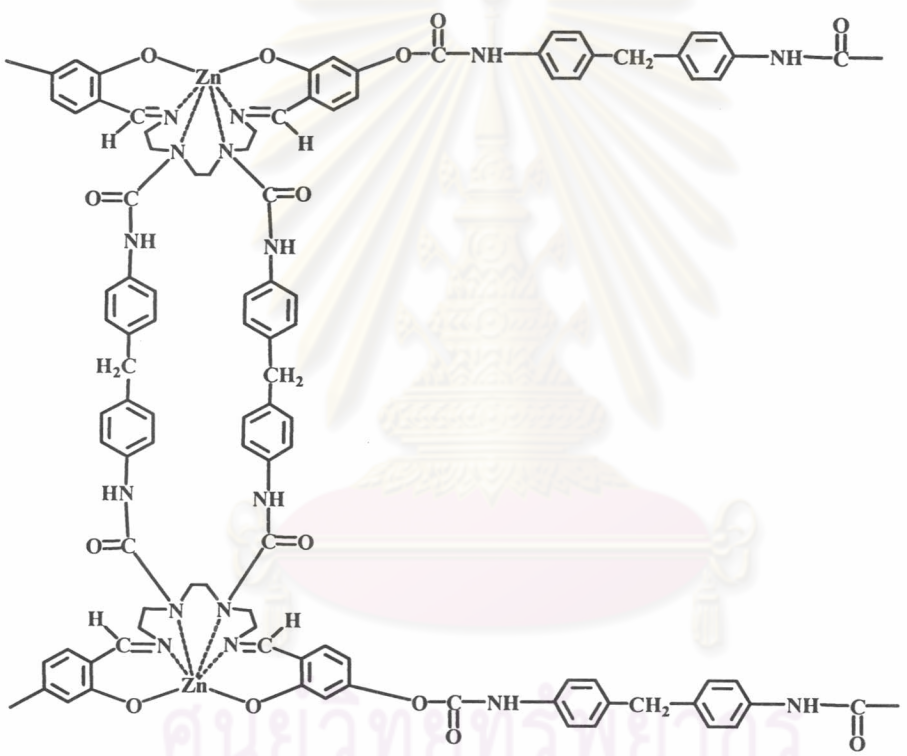

Figure 4.13 Possible crosslinked structure of ZnL-MDI (1:2)

From the solubility study, it was found that ZnL-MDI (1:2) was soluble in both DMF and DMSO. Therefore, it was more likely that the structure of ZnL-MDI (1:2) was linear rather than a crosslinked one.

4.2.2.3 Elemental analysis

The chemical structures of metal-containing polyurethane-ureas were confirmed by elemental analysis (Table 4.4). For ZnL-MDI (1:2) and NiL-MDI (1:2), the experimental value agreed with molecular formulas of $C_{50}H_{44}N_8O_7Zn$ and $C_{50}H_{44}N_8O_7Ni$, respectively. ZnL-PB (1:2) and NiL-PB (1:2) were also characterized by elemental analysis. However, their analytical data did not agree with the calculated data. This might be because the number of repeating units of PB prepolymer in both ZnL-PB (1:2) and NiL-PB (1:2) is an average value and therefore the formulas for each repeating unit of polymers are different. For the metal-containing polyurethane-ureas based on IPD, ZnL-IPD (1:2) and NiL-IPD (1:2), the elemental analysis was not done since these polymers were partially soluble in DMSO and this result from solubility data suggested that the obtained polymers were the mixture of linear and crosslinked polymers.

Table 4.4 Analytical data of metal-containing polyurethane-ureas

Polymers	Formula	Analytical data Found (Cald.)		
		C (%)	H (%)	N (%)
ZnL-MDI (1:2)	$C_{50}H_{44}N_8O_7Zn$	63.82 (64.27)	5.04 (4.75)	8.93 (11.99)
NiL-MDI (1:2)	$C_{50}H_{44}N_8O_7Ni$	64.00 (64.74)	5.05 (4.78)	10.80 (12.07)
ZnL-PB (1:2)	$C_{119}H_{178}N_{12}O_{15}Zn$	60.27 (62.07)	8.82 (7.74)	5.39 (7.81)
NiL-PB (1:2)	$C_{119}H_{178}N_{12}O_{15}Ni$	60.56 (62.26)	8.87 (7.75)	5.03 (7.83)

ศูนย์วิทยทรัพยากร
จุฬาลงกรณ์มหาวิทยาลัย

4.2.2.4 Solubility of metal-containing polyurethane-ureas

Solubility of metal-containing polyureas was tested in various polar and non-polar solvents (Table 4.5).

Table 4.5 Solubility data of metal-containing polyurethane-ureas[a]

Code	$CHCl_3$	CH_2Cl_2	CH_3CN	MeOH	THF	DMF	DMSO
ZnL-PUU							
ZnL-MDI (1:2)	-	-	-	-	-	++	++
ZnL-IPD (1:2)	-	-	-	-	-	-	+
ZnL-PB (1:2)	++	++	-	++	++	++	++
ZnL-PP (1:2)	++	++	-	++	++	++	++
NiL-PUU							
NiL-MDI (1:2)	-	-	-	-	-	++	++
NiL-IPD (1:2)	-	-	-	-	-	-	+
NiL-PB (1:2)	++	++	-	++	++	++	++
NiL-PP (1:2)	-	-	-	++	-	++	++

(-) insoluble; (+) partial soluble; (++) soluble

[a]10 mg sample was dissolved in 2 ml of a solvent

The solubility of zinc- and nickel-containing polyurethane-ureas was tested in various polar and non-polar solvents (Table 4.5). Most polyurethane-ureas were soluble in polar solvents such DMF and DMSO. These polymers were insoluble in $CHCl_3$, CH_2Cl_2, CH_3CN, MeOH and THF. The polymers based on prepolymers, namely ZnL-PB (1:2), ZnL-PP (1:2), NiL-PB (1:2) and NiL-PP (1:2), showed good solubility in DMF and DMSO and also soluble in some less polar solvents.

Since ZnL-IPD-12 and NiL-IPD-12 polymers were partial soluble in DMSO and the insoluble part of these polymers swelled in DMSO, therefore, these polymers contained the mixture of both linear and crosslinked polymers.

4.2.2.5 Inherent viscosity

The inherent viscosity all polyurethane-ureas was measured at 40°C in DMSO. The viscosity data of metal-containing polyurethane-urea are given in Table 4.6.

Table 4.6 Inherent viscosity of metal-containing polyurethane-ureas[a]

Polymer	η_{inh}
ZnL-PUU	
ZnL-MDI (1:2)	0.1648
ZnL-IPD (1:2)	0.0632
ZnL-PB (1:2)	0.2456
ZnL-PP (1:2)	0.1884
NiL-PUU	
NiL-MDI (1:2)	0.1566
NiL-IPD (1:2)	0.0675
NiL-PB (1:2)	0.2696
NiL-PP (1:2)	0.1454

[a]Determined at a concentration of 0.5g/100 ml in DMSO at 40°C .

The inherent viscosity of ZnL-IPD (1:2) and NiL-IPD (1:2) were found to be 0.06319 and 0.06747, respectively, which indicated that these polymers had relatively low molecular weight when compared to other metal-containing polyurethane-ureas. These polymers contained both linear and crosslinked polymers and therefore the soluble part should be the linear polymer with low molecular weight.

The viscosity of other metal-containing polyurethane-ureas was found to be in the range 0.1454-0.2696 dl/g. Comparing to the work of Jayakumar,[20] the inherent viscosity of calcium-containing polyurethane-ureas was found to be the range 0.0910-0.1090 dl/g, while the viscosity of nonmetal polyurethane-urea analogues was 0.1700-0.2710 dl/g. The lowering of the viscosity was explained that the ionic links in the polymer chain dissociated into low molecular weight fragments in polar solvents like DMSO. Therefore, the results indicated that the metal complex in the metal-containing polyurethane-ureas in this work does not dissociate in DMSO.

4.2.2.6 Thermogravimetric analysis

TGA curves and weight loss data of metal-containing polyurethane-ureas were shown in Figures 4.14-4.15 and Table 4.7-4.8, respectively. Initial decomposition temperature (IDT) of zinc- and nickel-containing polymers was found to be in the range 215-278 °C and 194-284 °C, respectively. The residual weight at 600 °C of zinc- and nickel-containing polymers was in the range 19 and 49, respectively. The residual weight at 900 °C of zinc- and nickel-containing polymers roughly corresponded to the amount of ZnO and NiO formed, respectively.

The difference in thermal stability of the polymers could be clearly observed at high temperature in the range 400-800 °C. Considering the wt% loss of polymers at 600 °C, the MDI-based polymers were more thermally stable than the polymers based on IPD, PB and PP. Part of the IPD-based polymers was low molecular weight linear chain and therefore the polymer was less thermally stable. The PB- and PP-based polymers contained aliphatic ether from PB and PP prepolymers, which caused the polymers to have good solubility in solvents but lower thermal stability.

Nickel-containing polymers showed better thermal stability than zinc-containing polymers. This result corresponded to the TGA result of the metal complexes, which indicated that NiL was more thermally stable than ZnL. Among all polymers, NiL-MDI-12 was the most thermally stable polymers.

Initial thermal degradation of polyurethane-ureas proceeded *via* urethane-ureas scission to give isocyanate and amine component (Scheme.4.4) [21].

ศูนย์วิทยทรัพยากร
จุฬาลงกรณ์มหาวิทยาลัย

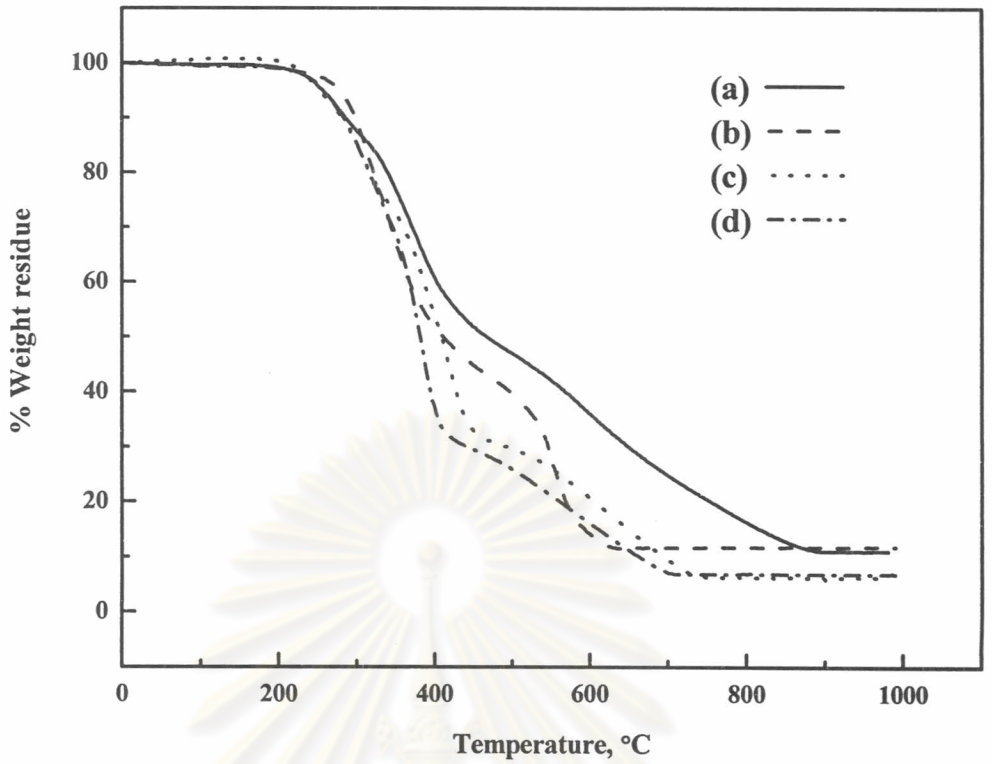

Figure 4.14 TGA thermogram of (a) ZnL-MDI (1:2); (b) ZnL-IPD (1:2); (c) ZnL-PB (1:2); (d) ZnL-PP (1:2).

Table 4.7 TGA data of zinc-containing polyurethane-ureas

Polymer	IDT (°C)	Weight loss (%) at different temperature (°C)							% Metal oxide
		300	400	500	600	700	800	900	
ZnL-MDI (1:2)	235	11	35	52	63	74	83	89	11.80
ZnL-IPD (1:2)	278	11	48	60	86	88	88	88	11.00
ZnL-PB (1:2)	215	15	45	70	79	91	94	94	6.18
ZnL-PP (1:2)	230	15	63	74	84	93	93	93	6.80

ศูนย์วิทยทรัพยากร
จุฬาลงกรณ์มหาวิทยาลัย

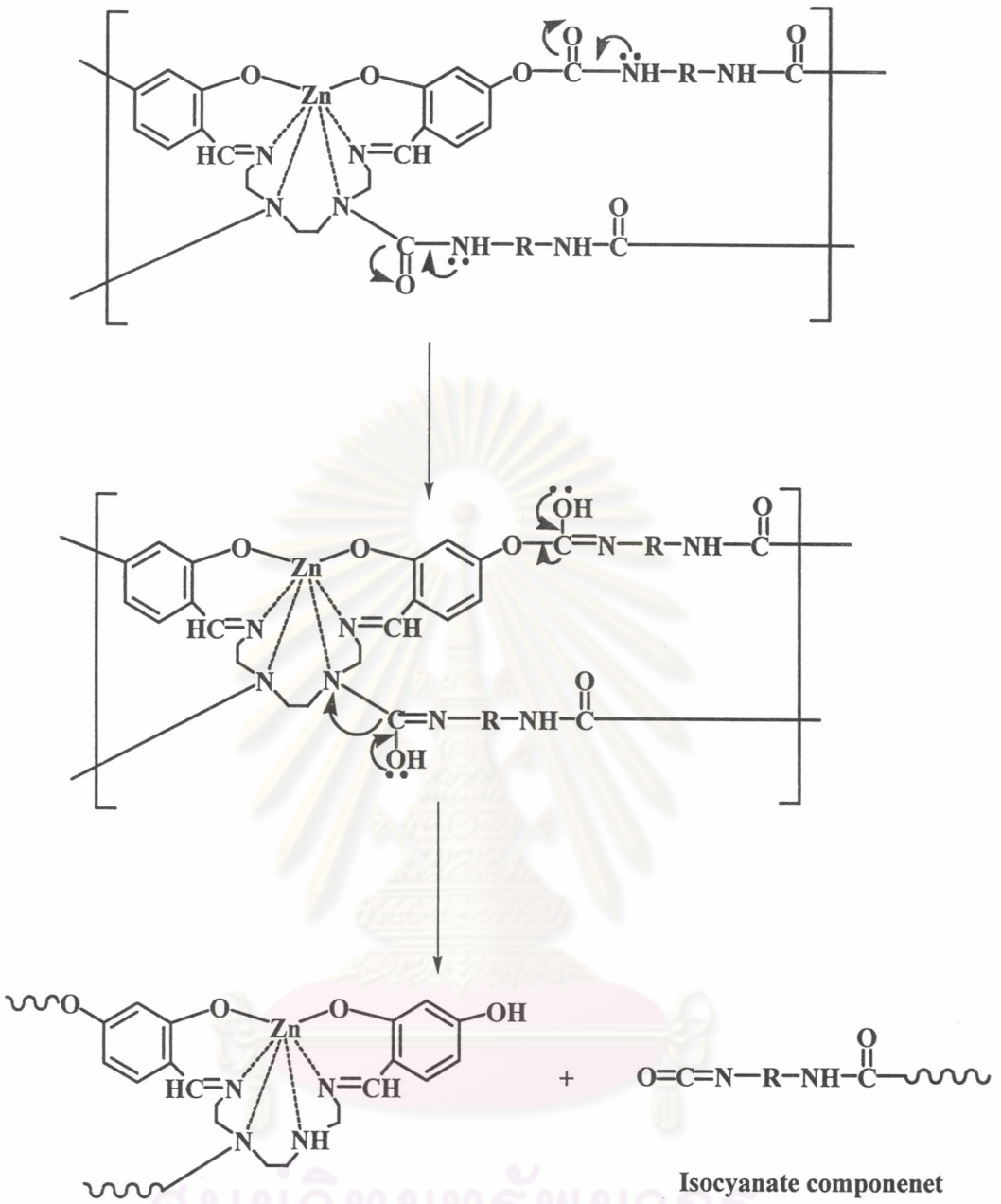

Scheme 4.4 Propose mechanism of degradation of metal-containing polyurethane-ureas

ศูนย์วิทยทรัพยากร
จุฬาลงกรณ์มหาวิทยาลัย

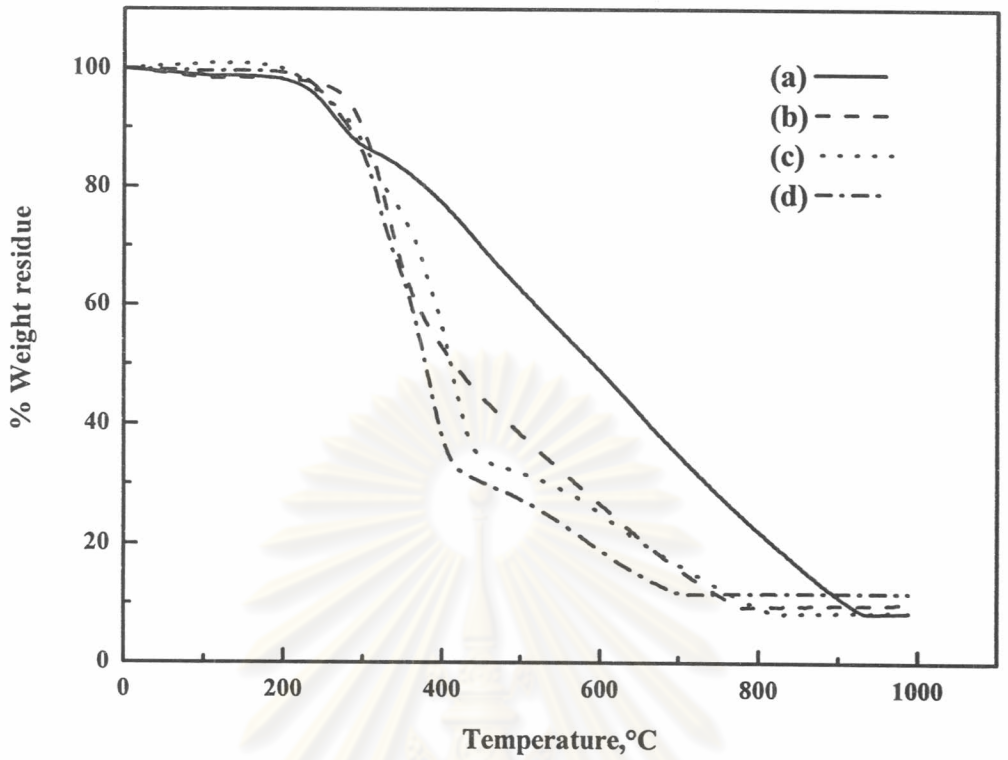

Figure 4.15 TGA thermogram of (a) NiL-MDI-12; (b) NiL-IPD-12; (c) NiL-PB-12; (d) NiL-PP-12

Table 4.8 TGA data of nickel-containing polyurethane-ureas

Polymer	IDT	Weight loss (%) at different temperature (°C)							% Metal oxide
	(°C)	300	400	500	600	700	800	900	
NiL-MDI (1:2)	226	13	23	37	51	65	78	89	8.46
NiL-IPD (1:2)	284	10	47	62	73	84	90	90	9.96
NiL-PB (1:2)	200	13	44	68	75	83	90	92	8.60
NiL-PP (1:2)	233	14	61	73	81	88	88	88	11.77

4.2.2.7 Flame retardancy

Flame-retardant properties of zinc- and nickel-containing polyurethane-ureas were compared from the limiting oxygen index (LOI) values as shown in Table 4.9

Table 4.9 LOI data of metal-containing polyurethane-ureas

Polymers	LOI
ZnL-PUU	
ZnL-MDI (1:2)	22.6
ZnL-IPD (1:2)	21.4
ZnL-PB (1:2)	24.3
ZnL-PP (1:2)	23.3
NiL-PUU	
NiL-MDI (1:2)	22.3
NiL-IPD (1:2)	21.4
NiL-PB (1:2)	23.7
NiL-PP (1:2)	23.3

Flame retardancy of both ZnL-PUU and NiL-PUU obtained from different diisocyanates showed almost the same value. LOI values of these polymers were in the range of 21.4-24.3. In comparison to the previous work reported by Chantarasiri[23], which described the synthesis, characterization and thermal properties of metal-containing polyurethane-ureas from hexadentate Shiff base metal complexes. The obtained polymers exhibited higher LOI values in the range 23-30.

ศูนย์วิทยทรัพยากร
จุฬาลงกรณ์มหาวิทยาลัย

4.2.2.8 UV-visible spectroscopy

UV-visible spectra and data of the metal-containing polyurethane-ureas are shown in Figures 4.16-4.17 and Tables 4.10-4.11, respectively. The absorption peaks of zinc-containing polyurethane-ureas showed two bands in the range 287-288 nm and 351-358 nm.

The absorption of nickel-containing polyurethane-ureas showed two absorption bands in the range 348-354 nm and 526 nm.

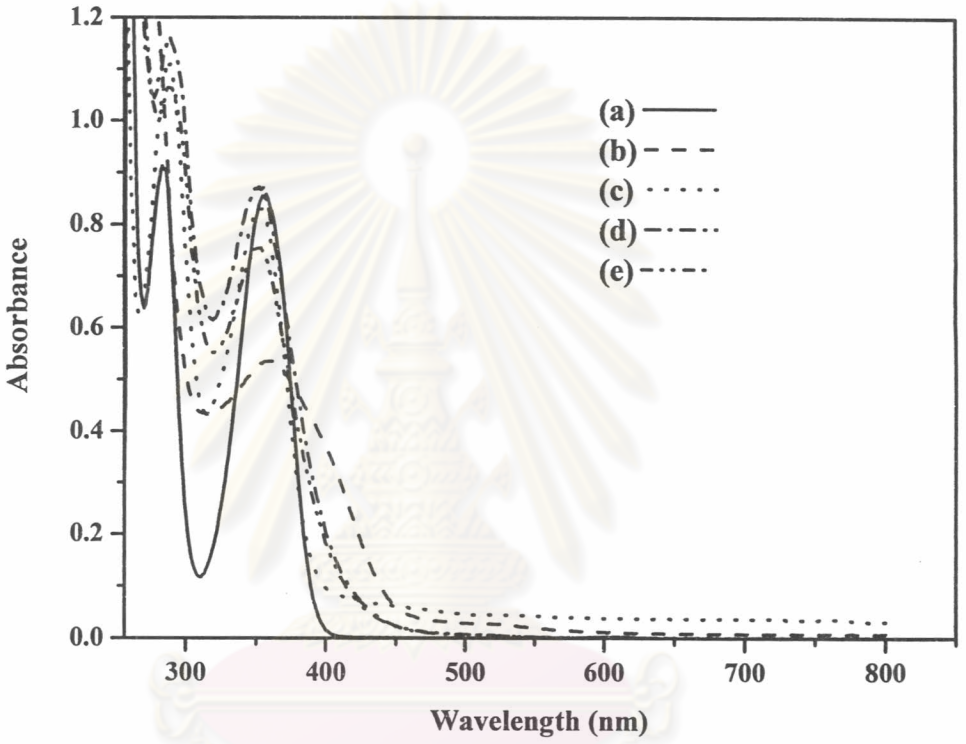

Figure 4.16 UV-visisble spectra of (a) ZnL; (b) ZnL-MDI (1:2); (c) ZnL-IPD (1:2); (d) ZnL-PB (1:2) and (e) ZnL-PP (1:2)

Table 4.10 UV-visible data of zinc-containing polyurethane-ureas in DMSO

Polymers	λ_{max} (nm)	Color in DMSO
ZnL	283, 357	Light yellow
ZnL-MDI (1:2)	358	Red-orange
ZnL-IPD (1:2)	287, 353	Deep yellow
ZnL-PB (1:2)	288, 351	Deep yellow
ZnL-PP (1:2)	287, 353	Deep yellow

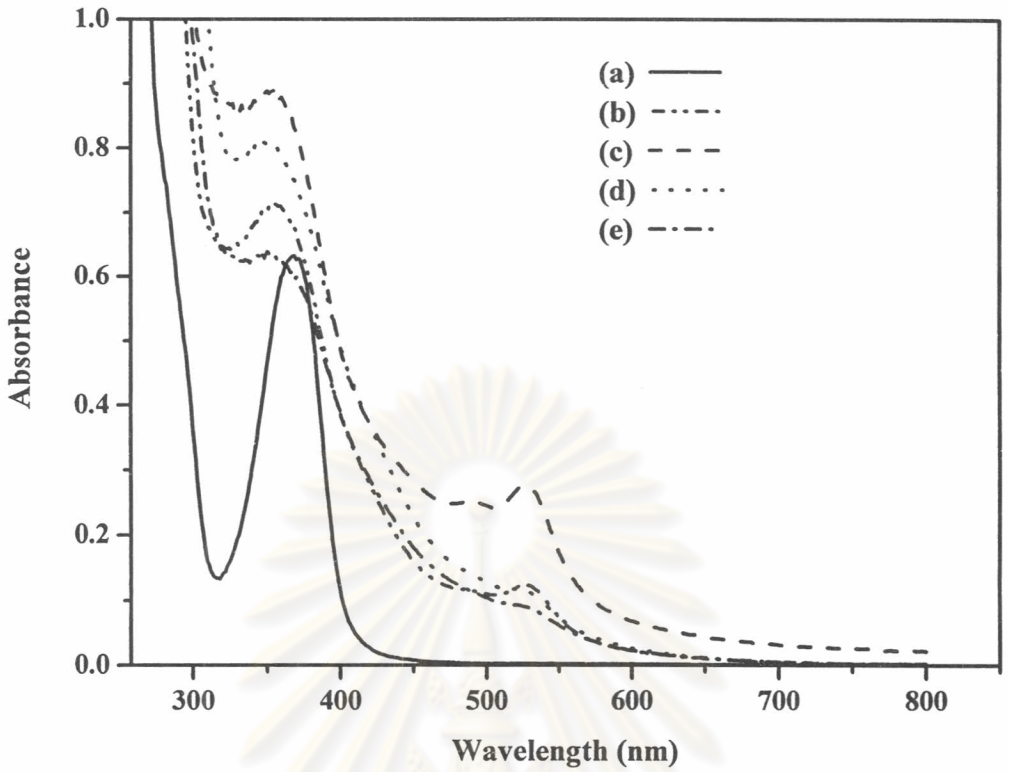

Figure 4.17 UV-visible spectra of (a) NiL; (b) NiL-MDI (1:2); (c) NiL-IPD (1:2); (d) NiL-PB (1;2) and (e) NiL-PP (1:2)

Table 4.11 UV-visible data of nickel-containing polyurethane-ureas in DMSO

Polymers	λ_{max} (nm)	Color in DMSO
NiL	368	Gray green
NiL-MDI (1:2)	354, 526	Red-brown
NiL-IPD (1:2)	353, 526	Red-brown
NiL-PB (1:2)	348	Red-brown
NiL-PP (1:2)	353	Red-brown

4.3 Synthesis of metal-containing copolyurethane-ureas (ML-coPUU) from the reaction between of ML, MDI and *m*-xylylenediamine

Metal-containing copolyurethane-ureas were synthesized from ML, MDI and *m*-xylylenediamine as shown in Scheme 4.5. MDI was chosen as diisocyanate in the synthesis since TGA data of the MDI-based polyurethane-ureas indicated that these polymers were the most thermally stable polymers when compared to the polymers obtained from other diisocyanates. The purpose of this work was to increase the urea linkage in the polymer structure by addition of *m*-xylylenediamine during the polymerization. It was expected that the polymers should have increased thermal stability due to more hydrogen bonding from the urea part and aromatic structure of diamine.

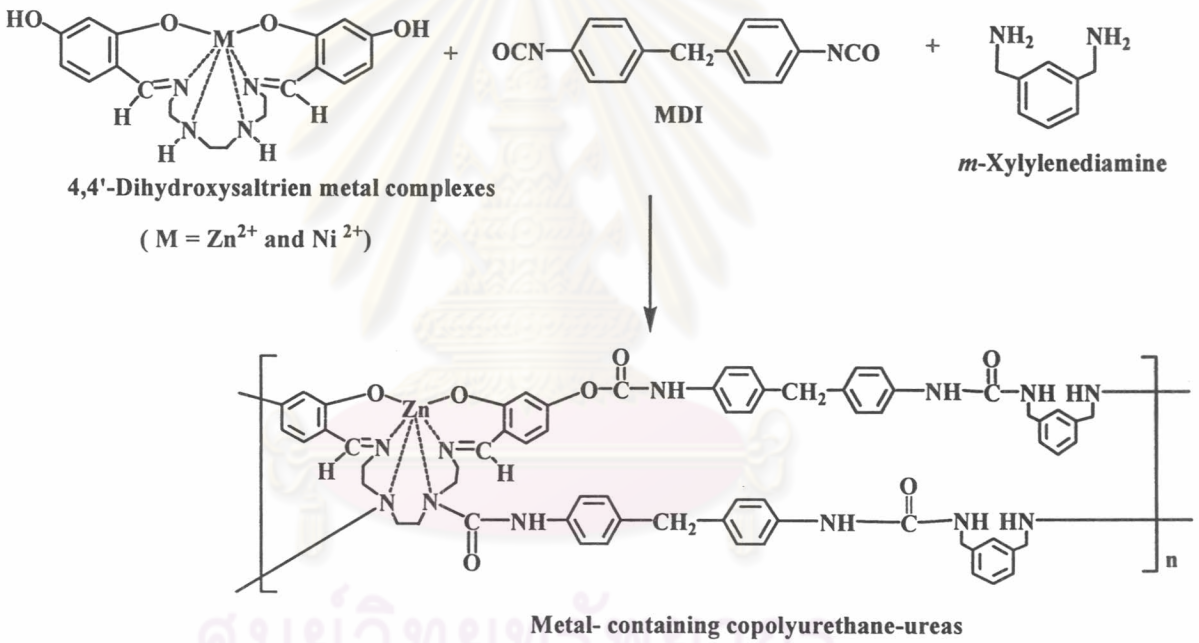

Scheme 4.5 The reaction between ML, MDI and *m*-xylylenediamine to yield metal-containing copolyurethane-ureas (ML-coPUU)

Table 4.12 The variable molar ratio components of ML-coPUU

ML	MDI	*m*-xylylenediamine	External appearance
ZnL			
0.5	3.0	1.5	Light yellow powder
1.0	3.0	1.0	Yellow powder
1.5	3.0	0.5	Orange yellow powder
NiL			
0.5	3.0	1.5	Brown powder
1.0	3.0	1.0	Yellow brown powder
1.5	3.0	0.5	Yellowish brown powder

The reaction between ML (M= Zn^{2+}, Ni^{2+}), MDI and *m*-xylylenediamine (D) at variable molar ratios of ML:MDI:D = 0.5:3.0:1.5, 1.0:3.0:1.0 and 1.5:3.0:0.5 was carried out in dried DMSO at 80-90 °C with DBTDL as a catalyst. The yields of zinc- and nickel-containing copolyurethane-ureas were in the range 87-97% and 81-91%, respectively.

The possible polymerization mechanism is that the amino and hydroxyl group in ML undergo reaction with isocyanate group in diisocyanate compounds to give urea and urethane linkages, respectively, while the amino group in *m*-xylylenediamine also undergoes a reaction with MDI to give urea linkage (Scheme 4.6).

ศูนย์วิทยทรัพยากร
จุฬาลงกรณ์มหาวิทยาลัย

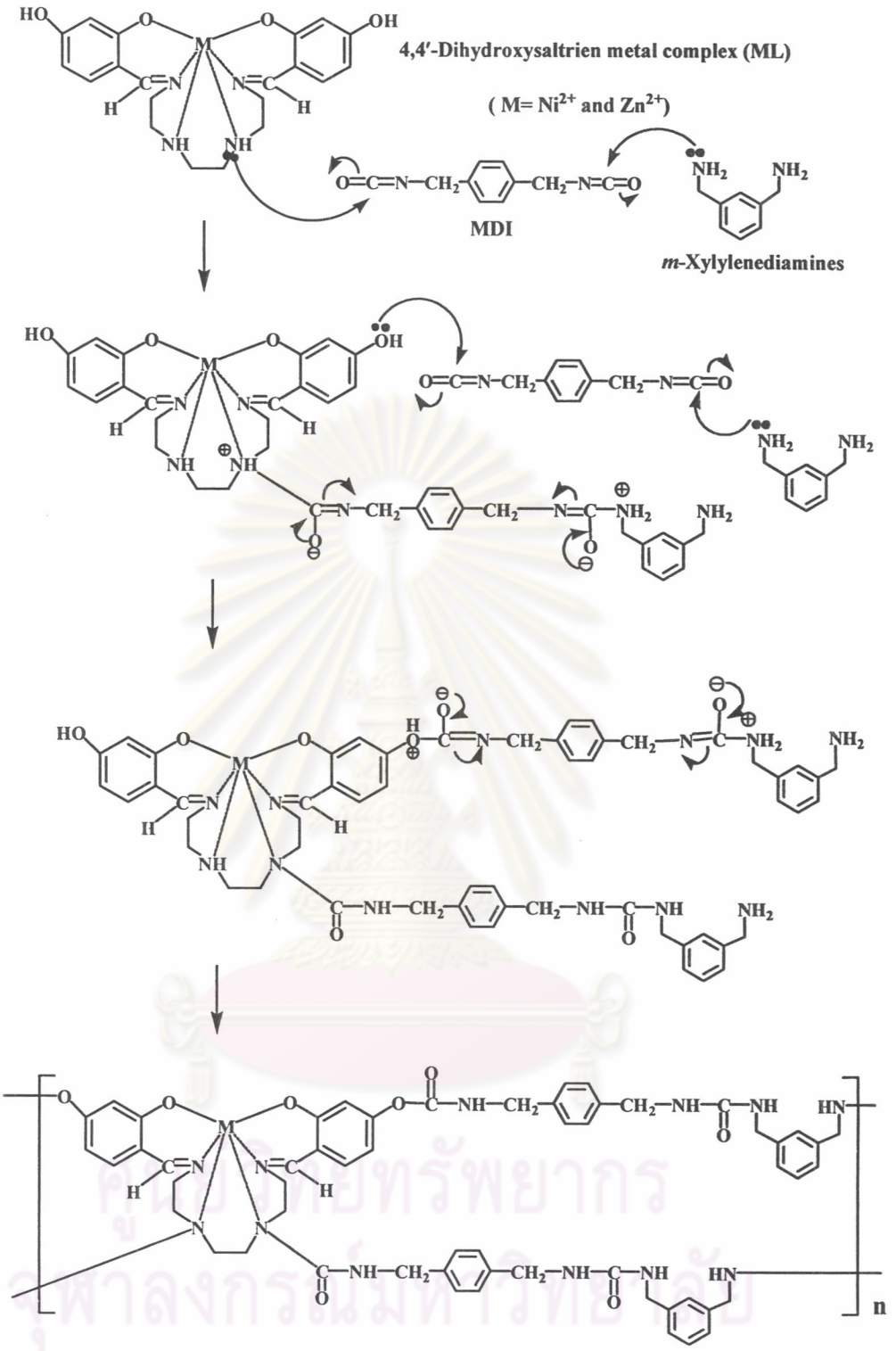

Scheme 4.6 Mechanism of the reaction between ML, MDI and *m*-xylylenediamine

4.3.1 Characterization of ML-coPUU

4.3.1.1 IR spectroscopy

IR spectra of zinc- and nickel-containing copolyurethane-ureas are shown in Figures 4.18 and 4.19, respectively.

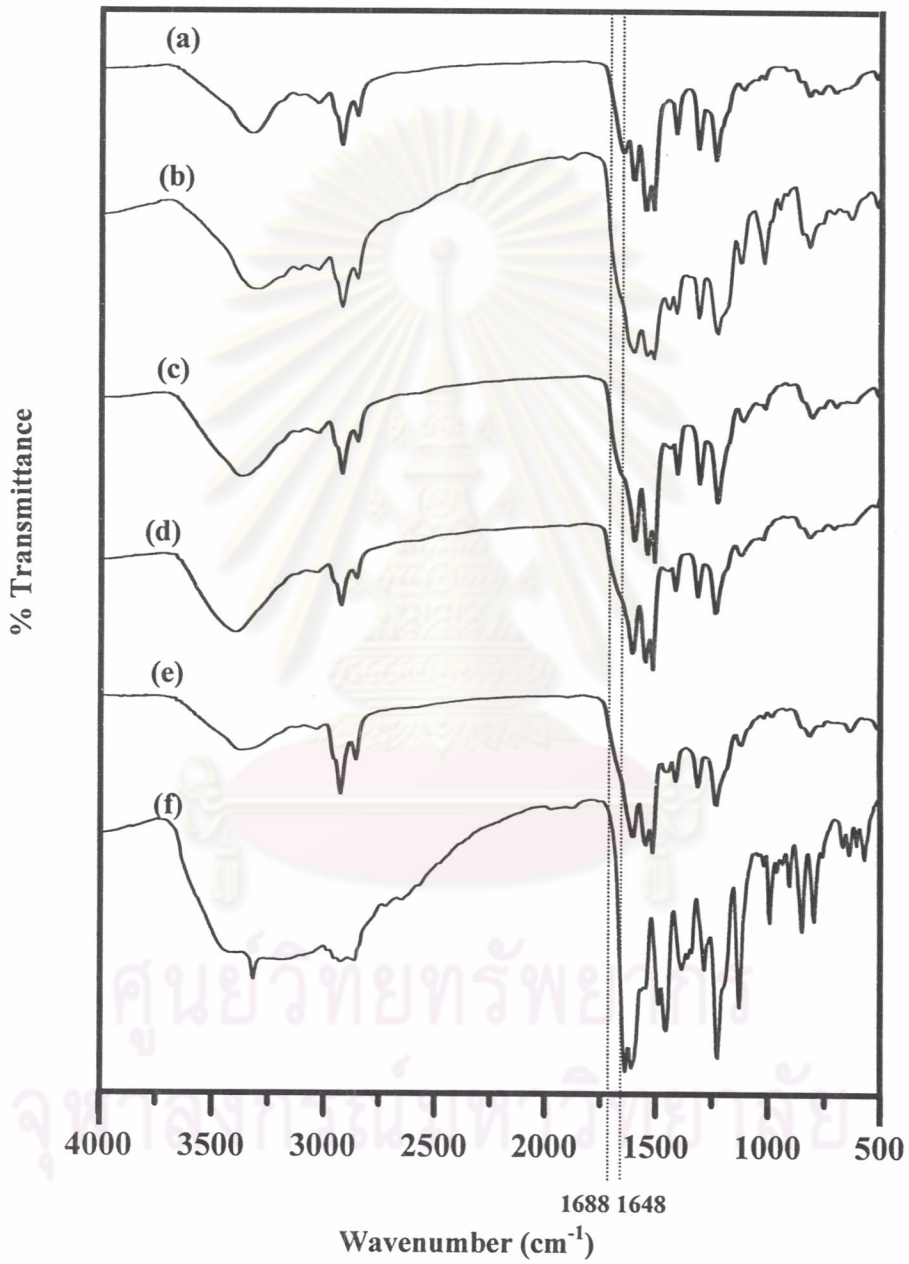

Figure 4.18 IR spectrum of (a) MDI-D; (b) ZnL-MDI (1:2); (c) ZnL-MDI-D (0.5:3.0:1.5); (d) ZnL-MDI-D (1.0:3.0:1.0); (e) ZnL-MDI-D (1.5:3.0:0.5); (f) ZnL

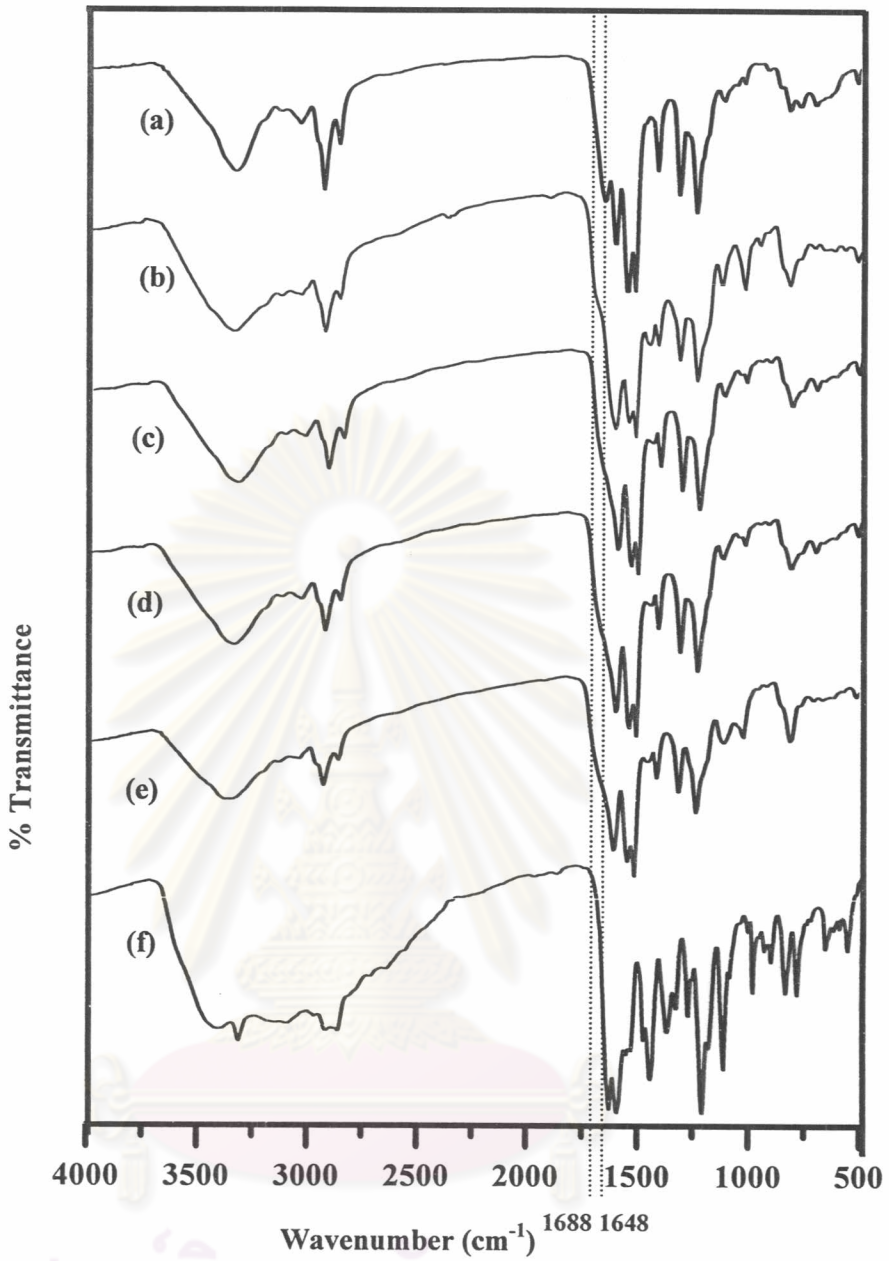

Figure 4.19 IR spectrum of (a) MDI-D; (b) NiL-MDI (1:2); (c) NiL-MDI-D (0.5:3.0:1.5); (d) NiL-MDI-D (1.0:3.0:1.0); (e) NiL-MDI-D (1.5:3.0:0.5); (f) NiL

Form Figure 4.18 (b-d), Figure 4.19 (b-d), all metal-containing copolyurethane-ureas have similar IR spectra. The important characteristic absorption bands are as follows: 3400-3300 cm^{-1} (N-H stretching), 2950-2800 cm^{-1} (aliphatic C-H stretching), the urethane-urea carbonyl that includes carbonyl absorption of ML-PUU is observed as a shoulder peak around 1688-1699 cm^{-1}, 1634-1600 cm^{-1} (imine C=N).

In comparison between ML with ML-coPUU and MDI-D with MnL-coPU, the result showed that the more content of *m*-xylylenediamine caused the more shoulder peak around 1648 cm^{-1} in ML-coPUU, which includes urea carbonyl absorption of MDI-D (Figures 4.18 and 4.19). The metal-containing copolymer that has the more content of ML is observed as a sharp peak around 1600 cm^{-1} and a characteristic peak of ML at 1450 cm^{1}.

4.3.1.2 Elemental analysis

The elemental analysis data of ZnL-MDI-D (1.0:3.0:1.0) and NiL-MDI-D (1.0:3.0:1.0) are given in Table 4.13. The elemental analysis data revealed that the experimentally determined percentage values of carbon and hydrogen are within the calculated values. However, the experimental percentage values of nitrogen disagreed with the calculated values. This might be due to the variation of molecular weight and structure of the copolymers. Therefore, the elemental analysis of the other metal-containing copolyurethane-ureas was not determined.

Table 4.13 Analytical data of ZnL-coPUU (ZnL-MDI-D (1.0:3.0:1.0)) and NiL-coPUU (NiL-MDI-D (1.0:3.0:1.0))

Polymers	Formula	Analytical data Found (Cald.)		
		C (%)	H (%)	N (%)
ZnL-coPUU (ZnL-MDI-D (1.0:3.0:1.0))	$C_{50}H_{44}N_8O_7Zn$	66.60 (66.89)	5.73 (5.15)	9.96 (13.00)
NiL-coPUU (NiL-MDI-D (1.0:3.0:1.0))	$C_{50}H_{44}N_8O_7Ni$	68.71 (67.24)	5.79 (5.17)	11.00 (13.07)

4.3.1.3 Solubility

Solubility test (Table 4.14) shows that these metal-containing copolyurethane-ureas were soluble in DMF and DMSO. These copolymers were insoluble in $CHCl_3$, CH_2Cl_2, CH_3CN, MeOH and THF.

Table 4.14 Solubility data of metal-containing copolyurethane-ureas[a]

Code	$CHCl_3$	CH_2Cl_2	CH_3CN	MeOH	THF	DMF	DMSO
ZnL-coPUU							
ZnL-MDI-D (0.5:3.0:1.5)	-	-	-	-	-	++	++
ZnL-MDI-D (1.0:3.0:1.0)	-	-	-	-	-	++	++
ZnL-MDI-D (1.5:3.0:0.5)	-	-	-	-	-	++	++
NiL-coPUU							
NiL-MDI-D (0.5:3.0:1.5)	-	-	-	-	-	++	++
NiL-MDI-D (1.0:3.0:1.0)	-	-	-	-	-	++	++
NiL-MDI-D (1.5:3.0:0.5)	-	-	-	-	-	++	++

(-) insoluble; (+) partial soluble; (++) soluble

[a]10 mg sample was dissolved in 2ml of a solvent

ศูนย์วิทยทรัพยากร
จุฬาลงกรณ์มหาวิทยาลัย

4.3.1.4 Inherent viscosity

The inherent viscosity all copolyurethane-ureas was measured at 40 °C in DMSO. The viscosity data are given in Table 4.15.

Table 4.15 Inherent viscosity of metal-containing copolyurethane-ureas

Polymer	η_{inh}
ZnL-PUU	
ZnL-MDI (1:2)	0.1648
ZnL-MDI-D (0.5:3.0:1.5)	0.2159
ZnL-MDI-D (1.0:3.0:1.0)	0.2159
ZnL-MDI-D (1.5:3.0:0.5)	0.1774
NiL-PUU	
NiL-MDI (1:2)	0.1566
NiL-MDI-D (0.5:3.0:1.5)	0.1355
NiL-MDI-D (1.0:3.0:1.0)	0.1197
NiL-MDI-D (1.5:3.0:0.5)	0.1647
MDI-D	0.1715

The data showed that the inherent viscosities were found to be in the range between 0.1197-0.1647 dl/g for NiL-coPUU series and 0.1774-0.2159 dl/g for ZnL-coPUU series. At the same molar ratio of ML: MDI: D in the copolymer and zinc-containing copolyurethane-ureas showed higher viscosity than nickel-containing copolyurethane-ureas. ZnL-coPUU series had the highest inherent viscosities, which was higher than that of ZnL-MDI (1:2). The amount of *m*-xylylenediamine in nickel containing copolyurethane-ureas did not affect the inherent viscosity value when that of compare with ML-MDI (1:2).

4.3.1.5 Thermalgravimetric analysis

TGA thermograms and weight loss data of zinc-containing copolyurethane-ureas were shown in Figure 4.20 and Table 4.16, respectively.

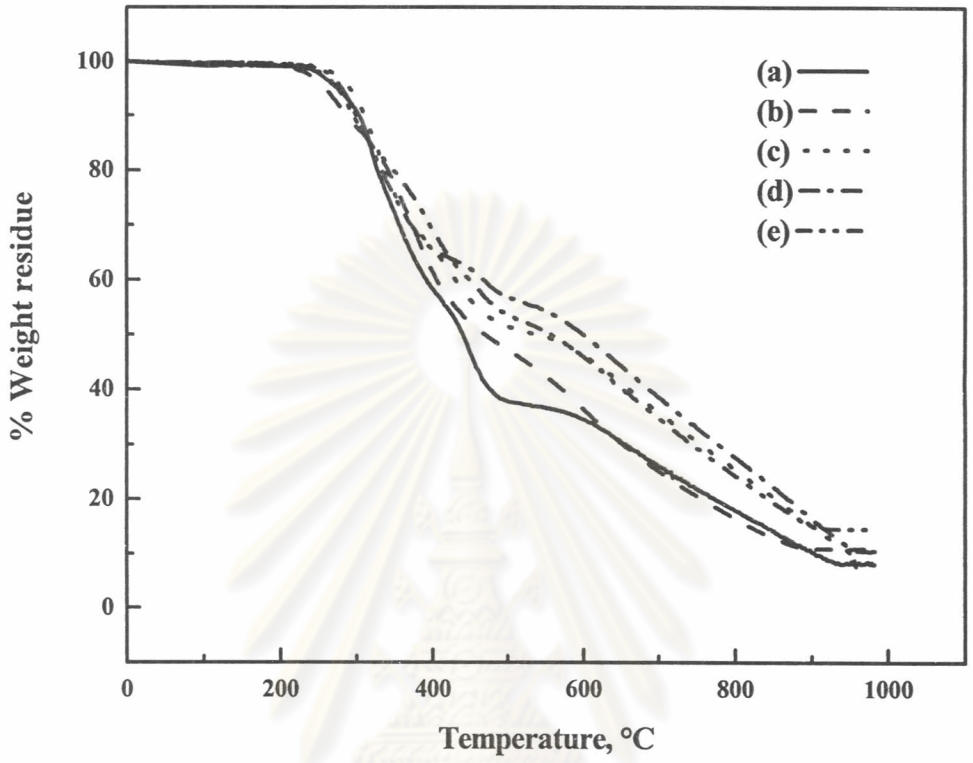

Figure 4.20 TGA thermogram of (a) MDI-D; (b) ZnL-MDI (1:2); (c) ZnL-MDI-D (0.5:3:1.5); (d) ZnL-MDI-D (1.0:3:1.0); (e) ZnL-MDI-D (1.5:3:0.5)

Table 4.16 TGA data of zinc-containing copolyurethane-ureas

Polymer	IDT (°C)	Weight loss (%) at different temperature (°C)							% Metal oxide
		300	400	500	600	700	800	900	
MDI-D	250	10	42	62	66	74	82	90	8.03
ZnL-MDI (1:2)	235	18	35	50	62	76	87	89	10.94
ZnL-MDI-D (0.5:3:1.5)	270	8	35	49	54	65	75	85	7.67
ZnL-MDI-D (1.0:3:1.0)	248	10	34	43	50	62	72	83	10.55
ZnL-MDI-D (1.5:3:0.5)	230	12	31	47	54	66	76	85	14.35

IDT of zinc-containing copolyurethane-ureas occurred in the temperature range 257-286 °C. Comparing to the polyurethane-ureas obtained from ZnL and MDI, the copolymers showed an increase in IDT when the amount of *m*-xylylenediamine in the copolymers was increased. ZnL-MDI-D (0.5:3.0:1.5) showed the highest IDT at 270 °C. The weight of residue at 600 °C of the copolymers also suggested that their thermal stability increase with increasing amount of *m*-xylylenediamine in the copolymers. ZnL-MDI-D (1.0:3.0:1.0) had the highest char yield of 50% at 600 °C, which was higher than that of ZnL-MDI (1:2). The theoretical amount of ZnO formed at 900 °C in the copolymers ZnL-MDI-D (0.5:3:1.5), ZnL-MDI-D (1.0:3:1.0) and ZnL-MDI-D (1.5:3:0.5) should be 3.38%, 6.77% and 10.15%, respectively. However, the residual weight at 900 °C obtained from TGA did not correspond to the amount of ZnO formed at this temperature.

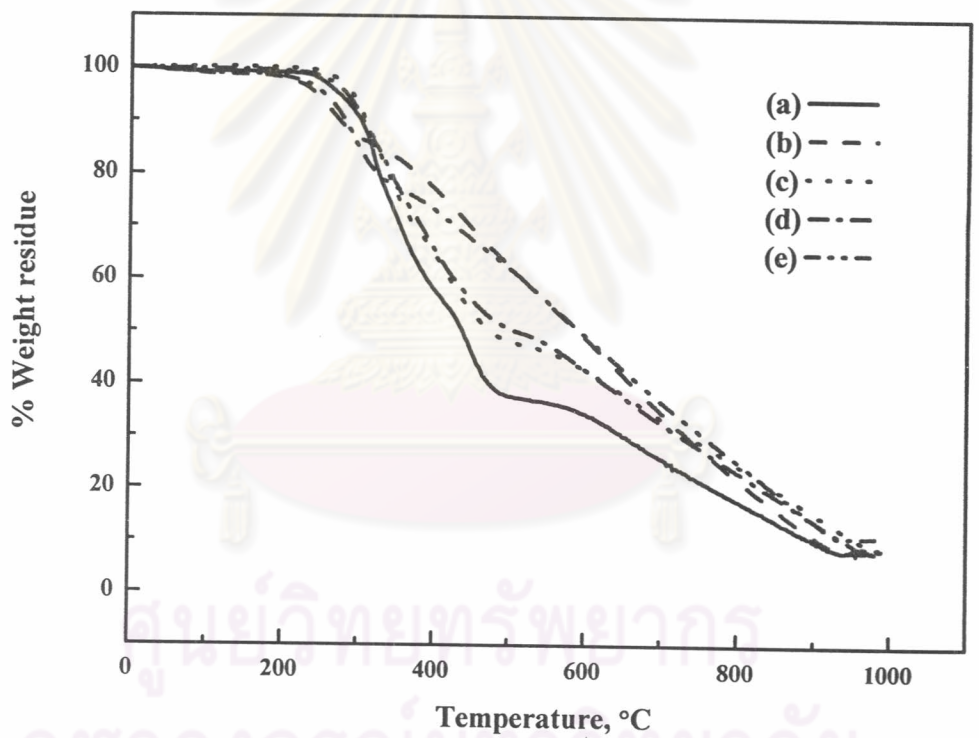

Figure 4.21 TGA thermogram of (a) MDI-D; (b) NiL-MDI (1:2); (c) NiL-MDI-D (0.5:3:1.5); (d) NiL-MDI-D (1.0:3:1.0); (e) NiL-MDI-D (1.5:3:0.5)

Table 4.17 TGA data of nickel-containing copolyurethane-ureas

Polymer	IDT (°C)	Weight loss (%) at different temperature (°C)							% Metal oxide
		300	400	500	600	700	800	900	
MDI-D	250	10	42	62	66	74	82	90	8.03
NiL-MDI-12	226	13	23	37	51	65	78	89	8.30
NiL-MDI-D-(0.5:3:1.5)	260	7	35	52	57	66	75	84	8.60
NiL-MDI-D-(1.0:3:1.0)	240	9	34	49	57	67	77	86	9.00
NiL-MDI-D-(1.5:3:0.5)	210	15	27	38	51	63	75	86	11.00

TGA curves and data of nickel-containing copolyurethane-ureas are given in Figure 4.21 and Table 4.17, respectively. The IDT values of nickel-containing copolyurethane-ureas followed the same trend as described in the case of zinc-containing copolyurethane-ureas that the IDT of the polymers increased with increasing amount of *m*-xylylenediamine. Increase in the amount of *m*-xylylenediamine in the nickel-containing copolyurethane-ureas did not affect the percentage of weight loss at 600 °C when compared to NiL-MDI (1:2). The theoretical amount of NiO formed at 900 °C in the copolymers NiL-MDI-D (0.5:3:1.5), NiL-MDI-D (1.0:3:1.0) and NiL-MDI-D (1.5:3:0.5) should be 3.125, 6.25% and 9.37%, respectively. However, the residual weight at 900 °C obtained from TGA did not correspond to the amount of NiO formed at this temperature.

ศูนย์วิทยทรัพยากร
จุฬาลงกรณ์มหาวิทยาลัย

4.3.1.6 Flame retardancy

Flame retardancy of the metal-containing copolyurethane-ureas was investigated by measuring their LOI values as shown in Table 4.18.

Table 4.18 LOI data of metal-containing copolyurethane-ureas

Polymers	LOI
ZnL-PUU	
ZnL-MDI-D (0.5:3.0:1.5)	23.3
ZnL-MDI-D (1.0:3.0:1.0)	23.3
ZnL-MDI-D (1.5:3.0:0.5)	23.5
NiL-PUU	
NiL-MDI-D (0.5:3.0:1.5)	23.8
NiL-MDI-D (1.0:3.0:1.0)	23.4
NiL-MDI-D (1.5:3.0:0.5)	23.3
MDI-D	22.2

All metal-containing copolyurethane-ureas showed the same LOI value. LOI value of the polymer without metal, MDI-D, synthesized from MDI and *m*-xylylenediamine was slightly lower than that of metal-containing polymers.

ศูนย์วิทยทรัพยากร
จุฬาลงกรณ์มหาวิทยาลัย

4.3.1.7 UV-visible spectroscopy

The UV-visible spectra and the absorption maxim values of the metal-containing copolyurethane-ureas are shown in Figures 4.22-4.23 and Tables 4.19-4.20, respectively. The absorbance peaks of zinc-containing copolyurethane-ureas had similar band to that of ZnL-MDI (1:2).

The absorption peaks of nickel-containing copolyurethane-ureas were different from those of NiL-MDI (1:2).

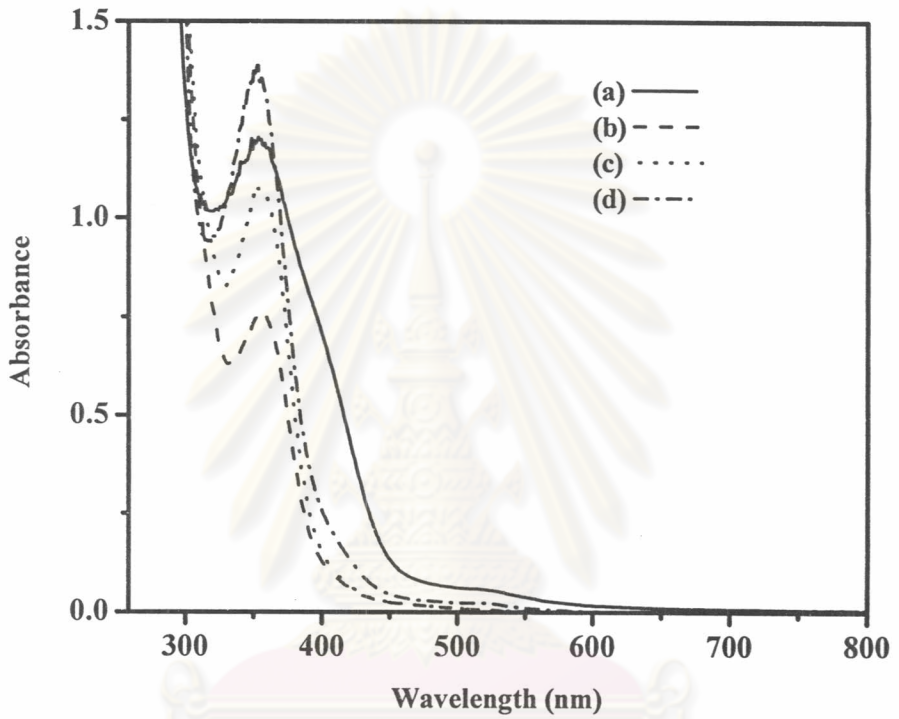

Figure 4.22 UV-visible spectra of (a) ZnL-MDI (1:2); (b) ZnL-MDI-D (0.5:3.0:1.5); (c) ZnL-MDI-D (1.0:3.0:1.0) and (d) ZnL-MDI-D (1.5:3.0:0.5)

Table 4.19 UV-visible data of the zinc-containing copolyurethane-ureas in DMSO

Polymers	λ_{max} (nm)	Color in DMSO
ZnL-MDI (1:2)	358	Red-orange
ZnL-MDI-D (0.5:3.0:1.5)	357	Light yellow
ZnL-MDI-D (1.0:3.0:1.0)	357	Light yellow
ZnL-MDI-D (1.5:3.0:0.5)	353	Light yellow

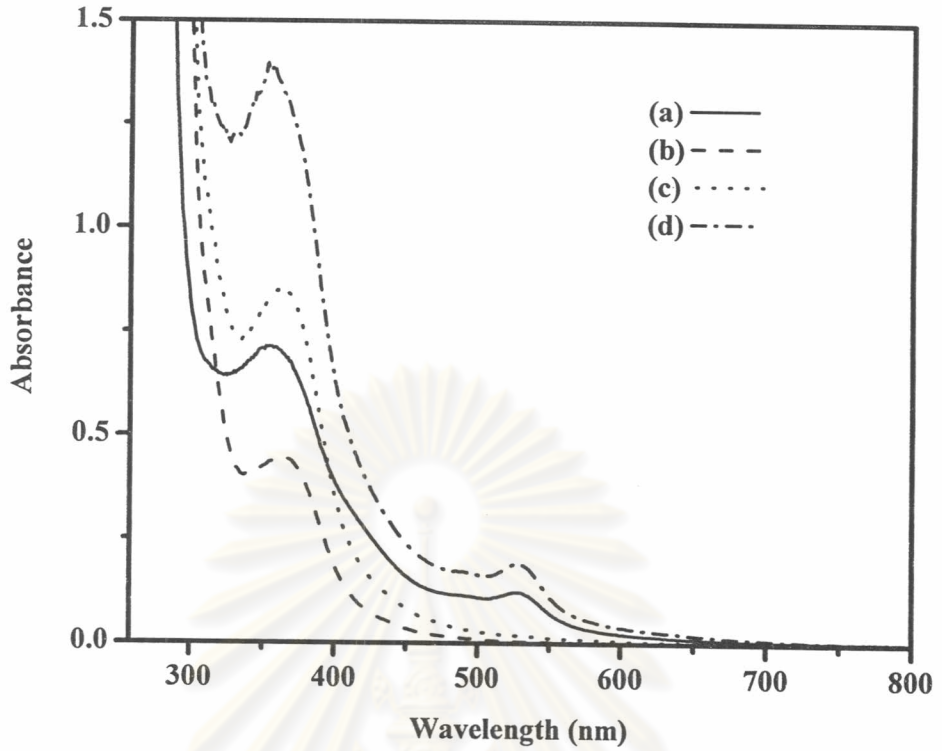

Figure 4.23 UV-visible spectra of (a) NiL-MDI (1:2); (b) NiL-MDI-D (0.5:3.0:1.5); (c) NiL-MDI-D (1.0:3.0:1.0) and (d) NiL-MDI-D (1.5:3.0:0.5)

Table 4.20 UV-visible data of the nickel-containing copolyurethane-ureas in DMSO

Polymers	λ_{max} (nm)	Color in DMSO
NiL-MDI (1:2)	354, 526	Red-brown
NiL-MDI-D (0.5:3.0:1.5)	362	Yellow-brown
NiL-MDI-D (1.0:3.0:1.0)	362	Yellow-brown
NiL-MDI-D (1.5:3.0:0.5)	351	Light yellow